Journal of Hydrology 627 (2023) 130462

Contents lists available at ScienceDirect

Journal of Hydrology

journal homepage: www.elsevier.com/locate/jhydrol

Unveiling an Environmental Drought Index and its applicability in the perspective of drought recognition amidst climate change

Aman Srivastava, Rajib Maity *

Department of Civil Engineering, Indian Institute of Technology Kharagpur, Kharagpur 721302, West Bengal, India

ARTICLE INFO

Keywords:
Climate Change
Environmental Droughts
Hydrological Modelling
Disaster Management
Hydroclimatology

ABSTRACT

As a complex natural disaster, drought encompasses significant and wide-ranging impacts on various environmental aspects. While meteorological, hydrological, agricultural, and socioeconomic droughts have been extensively studied, the scientific understanding of environmental droughts (the proposed fifth classification) remains relatively limited, hampering practical assessment efforts. To address this gap, the present study, for the first time, conducted a rigorous assessment of the applicability of a novel method, namely the heuristic method, in conjunction with a newly developed Environmental Drought Index (EDI). The present study thoroughly analyzed environmental drought events in India's Brahmani River basin, specifically focusing on the Jaraikela catchment. Firstly, the Minimum in-stream Flow Requirement (MFR) was determined using Tennant's method to synthetically estimate discharge rates to maintain the optimum flow range during the historical period (1980–2014). Secondly, Drought Duration Length (DDL) was calculated by counting consecutive water deficit months with negative monthly Streamflow Rate (SFR) and MFR differences. Three General Circulation Models (GCMs) output ensembles, namely EC-Earth3, MPI-ESM1-2-HR, and MRI-ESM2-0, participating in CMIP-6, were used for past (1980–2014) and future periods (FP-1: 2015–2022, FP-2: 2023–2045) under emission scenarios SSP245 and SSP585. The HydroClimatic Conceptual Streamflow (HCCS) model was employed to simulate the historical and future SFR. Thirdly, the largest water deficit magnitude during DDL was used to estimate the Water Shortage Level (WSL). Finally, integrating DDL and WSL provided the EDI for each environmental drought event. Results demonstrated a strong correspondence between the simulated EDI obtained using MPI-ESM1-2-HR under SSP585 and the observed EDI values, thereby indicating the credibility of the EDI in assessing environmental droughts. Furthermore, the study found severe droughts (i.e., EDI-3) dominating (71–73% of all droughts; occurring during non-monsoonal months) during FP-2 under SSP585 across all three GCMs, differing from moderate droughts in SSP245 of FP-2, both scenarios of FP-1, and the historical period. Based on the findings, the study finally proposed several adaptive measures to mitigate the impacts of increasing environmental drought events in the catchment.

1. Introduction

Droughts represent a complex interplay of climatic and hydrological factors, leading to prolonged periods of water scarcity. This sustained period of reduced water availability can result in hydrological extremes comparable to natural disasters such as floods (Chiang et al., 2021; Satoh et al., 2022). However, unlike floods, droughts manifest gradually, developing over an extended period and occasionally spanning entire continents [e.g., the "Millennium Drought" (2002–10) in Australia]. Far-reaching consequences of droughts underscore the need for robust understanding, monitoring, and mitigation strategies (Van Dijk et al., 2013; Yin et al., 2023). As traditionally classified, drought encompasses four distinct types: meteorological, agricultural, hydrological, and socioeconomic. These classifications recognize the interconnectedness of drought impacts across the hydrological cycle (Bae et al., 2019; Saha et al., 2022). However, recent studies, including the work of Crausbay et al. (2017) and Jiang et al. (2022), have highlighted the limitations of this traditional framework. They emphasize the need to incorporate ecological dimensions in drought definitions, recognizing that the traditional classification may overly prioritize human perspectives. Moreover, despite the significant impacts on ecosystems and human communities, current approaches to drought research,

* Corresponding author.
E-mail addresses: amansrivastava1397@kgpian.iitkgp.ac.in (A. Srivastava), rajib@civil.iitkgp.ac.in (R. Maity).

https://doi.org/10.1016/j.jhydrol.2023.130462
Received 3 August 2023; Received in revised form 19 October 2023; Accepted 26 October 2023
Available online 14 November 2023

management, and policy often overlook the evaluation of how drought explicitly affects ecosystems and the invaluable "natural capital" they offer. It is crucial to bridge this gap by integrating the understanding of drought's human and natural dimensions. By doing so, a vital step can be taken in effectively addressing the escalating risks of drought in the twenty-first century.

Crausbay et al. (2017) propose an expanded perspective by introducing the concept of ecological drought. This ecological drought is characterized as episodic periods of water scarcity that surpass the vulnerability thresholds of ecosystems, resulting in significant impacts on ecosystem services and triggering feedback mechanisms within natural and human systems. They emphasize the importance of considering the ecological consequences of drought, moving beyond solely human-centric viewpoints. In ecological drought, the deficit in available water is defined relative to the existing demand within a specific environmental system and region. This deficit is typically driven by climate variability processes, such as periods of below-normal precipitation or heightened Atmospheric Evaporative Demand (AED). For the first time, Vicente-Serrano et al. (2020) made a notable contribution by formally defining the concept of environmental drought. They adopted the definition of ecological drought put forth by Crausbay et al. (2017). However, they opted to use the term "environmental drought" instead, as they believed it better captures the integrated nature of human-environment interactions that underlie this type of drought. "Environmental" encompasses the intricate web of relationships among microbial fauna, animals, plants, soil characteristics, atmosphere, water, and human influences. It recognizes that human activities play a significant role in shaping the effects of drought on various ecosystems. Hence, using "environmental" instead of "ecological" in this study is driven by the desire to provide a more comprehensive and inclusive representation of the diverse range of effects and interactions. Additionally, this approach fosters a more rigorous and holistic examination of the consequences of drought, facilitating effective management strategies that consider both ecological and human dimensions (Crausbay et al., 2017; Jiang et al., 2022; Vicente-Serrano et al., 2020). Therefore, in the context of this study, environmental drought refers to a hydrological condition in river ecosystems where the available streamflow falls below critical levels necessary to sustain healthy aquatic habitats and meet the ecological requirements of the river. It is characterized by a scarcity of water resources that results in stress on river ecosystems, particularly with regard to aquatic life, water quality, and overall river eco-status. Coherently, environmental drought is specific to the impact of reduced streamflow on river ecosystems, and its evaluation is essential for understanding the health and resilience of these aquatic environments, especially within the context of changing climatic conditions and human interventions.

Environmental droughts are intricately connected to other types of drought, necessitating a holistic approach to their assessment. For instance, the meteorological, hydrological, and environmental dimensions of drought are interdependent, as soil hydrology profoundly influences the establishment and growth of vegetation. When vegetation is impacted by drought, such as through forest mortality or reduced biomass, it can alter hydrological processes, including rainfall interception, percolation, soil infiltration, and runoff. Consequently, these changes in vegetation and hydrology can significantly impact the availability of surface and subsurface water resources (Crausbay et al., 2017; Haile et al., 2020; Jiang et al., 2022; Vicente-Serrano et al., 2020; West et al., 2019). Moreover, environmental droughts exhibit strong associations with agriculture and socioeconomic droughts through various mechanisms. Ecosystems generate economically valuable products like timber, mushrooms, and pasture. Therefore, any losses or reductions in ecosystem productivity directly translate into economic losses. The impacts of environmental droughts on ecosystems can also have cascading effects on agriculture, where diminished ecosystem services, such as pollination and pest regulation, can adversely affect crop yields. Additionally, the availability and quality of water resources, influenced by environmental droughts and changing climate, directly impact agricultural production and livelihoods (Crausbay et al., 2017; Hagenlocher et al., 2019; Jiang et al., 2022; Shi et al., 2018; Srivastava et al., 2022a,b; Vicente-Serrano et al., 2020; Wang et al., 2022). Recognizing these interconnected relationships between environmental drought and meteorological, hydrological, agricultural, and socioeconomic droughts is crucial for a comprehensive understanding of drought dynamics. This interdisciplinary perspective is thus essential for effective drought management, policy formulation, and sustainable resource allocation, ensuring the resilience and well-being of natural ecosystems and human communities in the face of drought challenges.

Over the past several decades, significant efforts have been made to develop indices that can effectively quantify the severity of drought events. Some of the widely-used meteorological drought indices include the Palmer Drought Severity Index (PDSI) (Palmer, 1965), the Standardized Precipitation Index (SPI) (McKee et al., 1993), and the Standardized Precipitation Evapotranspiration Index (SPEI) (Vicente-Serrano et al., 2010); hydrological drought indices include Palmer Hydrological Drought Index (PHDI) (Karl, 1986), Surface Water Supply Index (SWSI) (Shafer & Dezman, 1982), and Standardized Runoff Index (SRI) (Shukla & Wood, 2008); agricultural drought indices include Crop Moisture Index (CMI) (Palmer, 1968), Crop Water Stress Index (CWSI) (Song et al., 2008), Relative Water Deficit (RWD) (Sivakumar et al., 2011), and Vegetation Condition Index (VCI) (Kogan, 1995); socioeconomic drought indices include the Multivariate Standardized Reliability and Resilience Index (MSRRI) (Mehran et al., 2015), Improved MSRRI (IMMSRI) (Guo et al., 2019), Socioeconomic Drought Index (SEDI) (Shi et al., 2018), Water Resources System Resilience Index (WRSRI) (Liu et al., 2020), and Standardized Water Supply and Demand Index (SWSDI) (Wang et al., 2022). One limitation of these indices is their oversight of the combined effects of drought duration length, severity of water shortage level, and environmental flow disparity when evaluating meteorological, hydrological, and agricultural droughts. While indices like SEDI and WRSRI have considered the first two factors for assessing socioeconomic droughts, the environmental perspective warrants further attention. Moreover, to the best of our knowledge, there is a notable lack of dedicated research on developing a new method and index for rationally identifying different degrees of environmental drought events considering the ecological condition of the stream/river. Therefore, a need is felt to extend research efforts toward developing indices specifically tailored for environmental drought.

In the context of advancing drought research and improving environmental management practices, this study seeks to establish a robust approach by developing a heuristic method and introducing the Environmental Drought Index (EDI). These approaches strive to be rooted in environmental flow assessment, given the scientific understanding of determining the appropriate quantity and quality of water required to necessarily sustain the ecosystem and protect water resources in a stream. The primary objective is thus to accurately identify environmental drought events across various severity levels (specifically, slight, moderate, severe, and extreme) by comprehensively assessing the combined influences of drought duration and water shortage levels, thereby determining the environmental flow requirements amidst climate change. By employing this novel methodology, the study aims to enhance the scientific rigor of environmental drought identification and analysis. Furthermore, this study will address strategies to mitigate the adverse effects of recurring drought events outside the monsoonal seasons by applying the heuristic method and EDI on the Jaraikela catchment of the Brahmani River basin in India as a case study. Considering the water supply and demand disparity, the proposed method and index prioritize streamflow as the primary input. In the present study, historical drought analysis uses observed data, thereby validating the new method's practicality and index. Additionally, future drought analysis incorporates multiple General Circulation Model (GCM) datasets under moderate and high emissions pathways. This approach allows for the assessment of a diverse range of potential drought conditions anticipated in the future. Overall, the introduced method and index (EDI) offer a more holistic understanding of environmental drought within the context of climate change. This knowledge is vital for decision-makers as they evaluate climate change's repercussions on water resource management, particularly concerning the overall environmental water balance.

2. Methods and methodology

2.1. HCCS model development

The HydroClimatic Conceptual Streamflow (HCCS) model, developed by Bhagwat and Maity (2014) and further improved by Suman and Maity (2019), is a conceptual model designed to incorporate the time-varying nature of watersheds and utilize daily climatic inputs, such as rainfall and air temperature, to predict daily streamflows (refer to Fig. S1). The conceptual framework of the HCCS model assumes a relationship between key hydrological components, including evapotranspiration and groundwater recharge, and water availability in near-surface strata at any given time. This availability, the System Wetness Condition (SWC; at time t is $V(t)$), captures the temporal variations of the watershed's hydrological behavior. Moreover, the HCCS model recognizes that the maximum value of the SWC (V_{max}) can also vary with time, albeit at a slower rate than $V(t)$. This adjustment accounts for the influence of climate change and the characteristics specific to the watershed. By considering the time-varying properties of the watershed, the HCCS model becomes a valuable tool for assessing future variations in streamflow under changing climate conditions. The main governing equation of the HCCS model is shown in Eqs (1) and (2). Readers can refer to Bhagwat and Maity (2014) and Suman and Maity (2019) for details on the step-wise development of the HCCS and improved HCCS model, respectively.

$$\frac{B[\{S(t+1)\}^b - \{S(t)\}^b}{\Delta t} = P(t) - E_p t - \frac{B[S(t)]^b}{V_{max}} - S(t) - k[S(t)]^b \tag{1}$$

$$S(t+1) = \left[\{S(t)\}^b + \frac{\Delta t}{B}\left\{P(t) - E_p(t) - \frac{B[S(t)]^b}{V_{max}} - S(t) - k[S(t)]^b\right\}\right]^{1/b} \tag{2}$$

Eqs. (1) and (2) provide information on several parameters that define the dynamics of the catchment. The precipitation depth over the watershed, denoted as $P(t)$, and the potential evapotranspiration loss from the catchment, represented by $E_p(t)$, are considered in the calculations. Additionally, the streamflow divided by the catchment area, denoted as $S(t)$, is considered. The four key parameters used to describe the catchment are B, b, k, and $V_{\max}$. The system wetness condition, $V(t)$, is conceptualized as the amount of water stored in the near-surface layers of the entire watershed, encompassing depression storage, soil water retention, reservoir storage, and other relevant factors. $V_{\max}$ represents the maximum values of the system wetness condition for the watershed, while $S_{\max}$ denotes the physically feasible maximum streamflow at the watershed's outlet. Parameter B is influenced by both $V_{\max}$ and $S_{\max}$, capturing their interrelationship. The nonlinearity between $S(t)/S_{max}$ and $V(t)/V_{max}$ is quantified by the inverse of parameter b. $S(t)$ and $V(t)$ refer to the streamflow and system wetness conditions at a given time step. Parameter k is a dimensionless value that signifies the basin-averaged contribution to groundwater recharge. Together, these parameters provide a comprehensive understanding of the catchment's hydrological characteristics. The parameter k is a unit less value that indicates the basin-averaged contribution to groundwater recharge.

This study's HCCS model was methodically developed to simulate observed Streamflow Rate (SFR) data (refer to Fig. S1). The calibration period spanned from 1980 to 2007, while the subsequent validation period covered 2008 to 2014. The model's robustness and reliability were ensured by accurately replicating streamflow patterns during these periods. To provide insights into future streamflow dynamics, the HCCS model was further employed to generate predicted streamflows from 2015 to 2045. In order to effectively analyze and validate these predictions, the future period was divided into two distinct phases. The first phase, Future Period One (FP-1), encompassed 2015 to 2022. This phase facilitated the validation of the simulated EDI values by comparing them against observed EDI values, thereby ensuring the reliability of the model's performance and EDI during the initial future period. The second phase, Future Period Two (FP-2), extended from 2023 to 2045. This division was undertaken considering the comprehensive scope of the study and its potential implications. Notably, the study extended the investigation period until 2045 to align with the Indian Government's Technology Vision (TV), which aims to devise environmental solutions until 2047 (TV2047 in line with TV2020 and TV2035: https://tifac.org.in/index.php/reports-publications/reports-2010-onwards/tv-2035-reports-2, accessed July 2023), commemorating 100 years of India's independence. Consequently, the study's findings are relevant as they can offer valuable guidance on drought monitoring and management strategies, aligning with the nation's long-term vision.

2.2. Minimum in-stream flow Requirement (MFR) estimation: Tennant's method

Tennant's method, also known as the Montana method, was initially developed in the United States in 1975 by Tennant (1976). Originally designed for trout conservation, this method is based on extensive field observations conducted in the mid-west region of the USA. It provides guidelines for flow management based on the percentage of Mean Annual Flow (MAF) rate, catering to seven distinct levels of river eco-status, namely (1) Optimum range of flow, (2) Outstanding habitat, (3) Excellent habitat, (4) Good habitat, (5) Fair and degrading habitat, (6) Poor or minimum habitat, and (7) Severe degradation. Since its inception, the method has undergone refinements and is currently applied globally for Environmental Flow Assessment (EFA) purposes. More specifically, the Tennant method adopts a seasonal approach, dividing the water year into two halves: the High Flow Season (HFS) and the Low Flow Season (LFS). For each season, specific flow thresholds are recommended as a percentage of the MAF rate, aiming to achieve desired levels of eco-status. It is important to note that the method primarily relies on hydrological data and incorporates subjective assessments. As a result, it is particularly suitable for preliminary studies and situations with minimal controversy. Detailed guidelines for Environmental Flow Requirements (EFR) based on Tennant's method can be found in Tennant (1976).

The Minimum in-stream Flow Requirement (MFR) of the Jaraikela catchment in the present study (detailed in Section 3.1) was determined using Tennant's method (detailed in Table 1) by analyzing the observed SFR data spanning 35 years from 1980 to 2014. This study defines MFR as the minimum in-streamflow level (threshold value) necessary to sustain and support the river basin's various ecological/environmental functions coherent with Tennant's environmental flow description. This includes maintaining vital ecological processes, such as aquatic habitat preservation, water quality maintenance, sediment transport, and overall ecosystem health. Establishing the MFR makes it possible to strike a balance between water resource utilization and the protection of the river's ecological integrity, fostering sustainable water management practices within the basin/catchment. To understand the eco-status comprehensively, the present study followed the definition of HFS and LFS as defined in the Tennant method. The period of the year when river flow conditions are relatively high and not affected by drought or significant water scarcity is considered the HFS. This season provides a baseline for understanding the ecological needs of the river and the aquatic ecosystems it supports when water availability is relatively abundant. This season typically occurs during months when there is a surplus of water in the river, often associated with rainfall and snowmelt

Table 1
Calculation of monthly average Minimum in-stream Flow Requirement (MFR) for Jaraikela catchment using Tennant's method.

Month	No. of days	Mean Monthly Flow Volume for 1980–2014 (cumec.day)	MFR in the month (cumec.day) (for Good Habitat) In HFS[2] @40% of MAF (=137.07 cumecs)	In LFS[3] @20% of MAF (=137.07 cumecs)	Flushing flows[1] in the month (cumec.day)	Total MFR volume in the month (cumec.day) $[= d + e + f]$	Mean Streamflow Rate (SFR) (cumecs) $[= c/b]$	Mean MFR rate (cumecs) $[= g/b]$
a	b	c	d	e	f	g	h	i
January	31	563.16		849.85		849.85	18.17	27.41
February	28	366.44		767.61		767.61	13.09	27.41
March	31	263.25		849.85		849.85	8.49	27.41
April	30	154.04		822.44		822.44	5.13	27.41
May	31	240.53		849.85		849.85	7.76	27.41
June	30	3692.81	1644.88			1644.88	123.09	54.83
July	31	11003.40	1699.71			1699.71	354.95	54.83
August	31	14777.67	1699.71		274.15	1973.85	476.70	63.67
September	30	11996.55	1644.88			1644.88	399.88	54.83
October	31	4782.04	1699.71			1699.71	154.26	54.83
November	30	1490.65		822.44		822.44	49.69	27.41
December	31	701.12		849.85		849.85	22.62	27.41
Total	365	50031.65						

[1] Flushing flow of 200 % MAF (Mean Annual Flow $= \frac{50031.65}{365} = 137.07$) is considered for the month of August.
[2] High Flow Season (HFS; from June to October).
[3] Low Flow Season (LFS; from November to the following May).

in the watershed. While LFS refers to a period of the year when river flow conditions are relatively low or when the river experiences drought or significant water scarcity. This season typically occurs during months when there is a deficit of water in the river, often associated with reduced rainfall and minimal runoff in the watershed. Considering the literature on the Jaraikela catchment in specific and the Brahmani River basin in general on hydroclimatological features [discussed in detail in Section 3.1 and by Amrit et al. (2018), Islam et al. (2012), Sinha et al. (2020), Swain et al. (2020), Swain et al. (2021), Vandana et al. (2019)] and by adhering to the definitions of HFS and LFS as described above, the HFS was defined from June to October, while the LFS encompassed the months from November to May. Although the southwest monsoon typically concludes by September (June to September, as defined by the India Meteorological Department), it's noteworthy that there remains ample streamflow in the subsequent month, i.e., October, and thus this study considered HFS until October. Drawing from existing literature, Tennant's qualitative descriptor of "Good Habitat" for the Koel River was adopted as the target eco-status for the Jaraikela catchment. To attain this level, the study followed Tennant's Table (Tennant, 1976), which recommends streamflow thresholds as a percentage of the MAF rate. Accordingly, 40% of the MAF rate was prescribed during the HFS, while 20% of the MAF rate was suggested during the LFS. Additionally, a flushing flow of 200% of the MAF rate, lasting between 48 and 96 hours, was explicitly implemented in August during the HFS. Importantly, the selection of the month (in HFS) for the flushing flow considered the need to avoid singularly relying on the flushing flow as the sole determinant of the specific type of environmental drought. By compiling monthly values for the average water year, the study aggregated the flows during the HFS, LFS, and flushing flows to determine the MFR for the Koel River in the Jaraikela catchment (refer to Table 1). Subsequently, a flow hydrograph representing the monthly average SFR and the monthly average MFR was generated, providing a comprehensive visualization of the flow dynamics within the catchment.

2.3. Heuristic method for EDI development

As previously mentioned, the main aim of this study was to develop a heuristic method and EDI specifically for the Jaraikela catchment within the Brahmani River basin. To achieve this objective, the study rigorously followed the detailed methodology outlined in Fig. 1. This methodology encompassed crucial steps such as utilizing the output of the HCCS model, comparing SFR with MFR, and establishing the definitions of drought duration and water shortage lengths (i.e., DDL and WSL) to ultimately construct the EDI. In designing the methodology, this study also drew upon the work of Shi et al. (2018), who developed the SEDI – 'Socioeconomic Drought Index'. By incorporating the approaches from this research, the present study ensured a scientifically rigorous framework for developing the heuristic method and EDI.

First, a comprehensive analysis was conducted by comparing the MFR, determined using Tennant's method (detailed in Section 2.2), with both the observed SFR and the projected/simulated SFR obtained through applying the HCCS model (detailed in Section 2.1). This comparison encompassed the observed period from 1980 to 2014 and the future periods of 2015 to 2022[1] and 2023 to 2045. The comparison between the monthly SFR and MFR served as a valuable indicator of environmental drought magnitude. Specifically, a negative difference (monthly difference less than zero), also defined in this study as a water deficit, signified that the SFR for that particular month was insufficient to meet the minimum environmental flow requirements. Consequently, these identified months were classified as environmental drought months. It is important to note that an environmental drought event persisted until the monthly difference between SFR and MFR became non-negative. To quantify the duration of environmental drought, this study introduces the concept of Drought Duration Length (DDL), which represents the continuous number of months characterized by

[1] The first Future Period (FP-1: 2015–2022) is designated as the "future period," given that the study accessed observed data from 2015 to 2018, with which the study could perform rigorous validation by comparing the observed datasets/outputs (SFR and EDI) from 2015 to 2018 with the simulated datasets/outputs (HCCS-modeled simulated SFR and heuristic method-based simulated EDI) within FP-1. This step ensured that the simulated outputs accurately aligned with the observed values. Furthermore, the temporal framework employed in this study adheres to the established conventions outlined by the CMIP6 guidelines for data users. CMIP6 demarcates the historical period, encompassing data up to 2014, and designates the simulated or future period, commencing from 2015 onward (refer to the list of published papers on CMIP6: https://cmip-publications.llnl.gov/view/CMIP6/, accessed in November 2023). Accordingly, this study has classified 1980–2014 as the historical period, and the timeframe spanning 2015–2045 is referred to as the Future Period (FP). The FP has been further subdivided into two distinct categories: FP-1, comprising 2015–2022, and FP-2, spanning 2023–2045. It's imperative to clarify that FP-1 should not be misconstrued as part of the historical period; it is a product of CMIP6 model simulations and is, therefore, regarded as a future period, notwithstanding the passage of time.

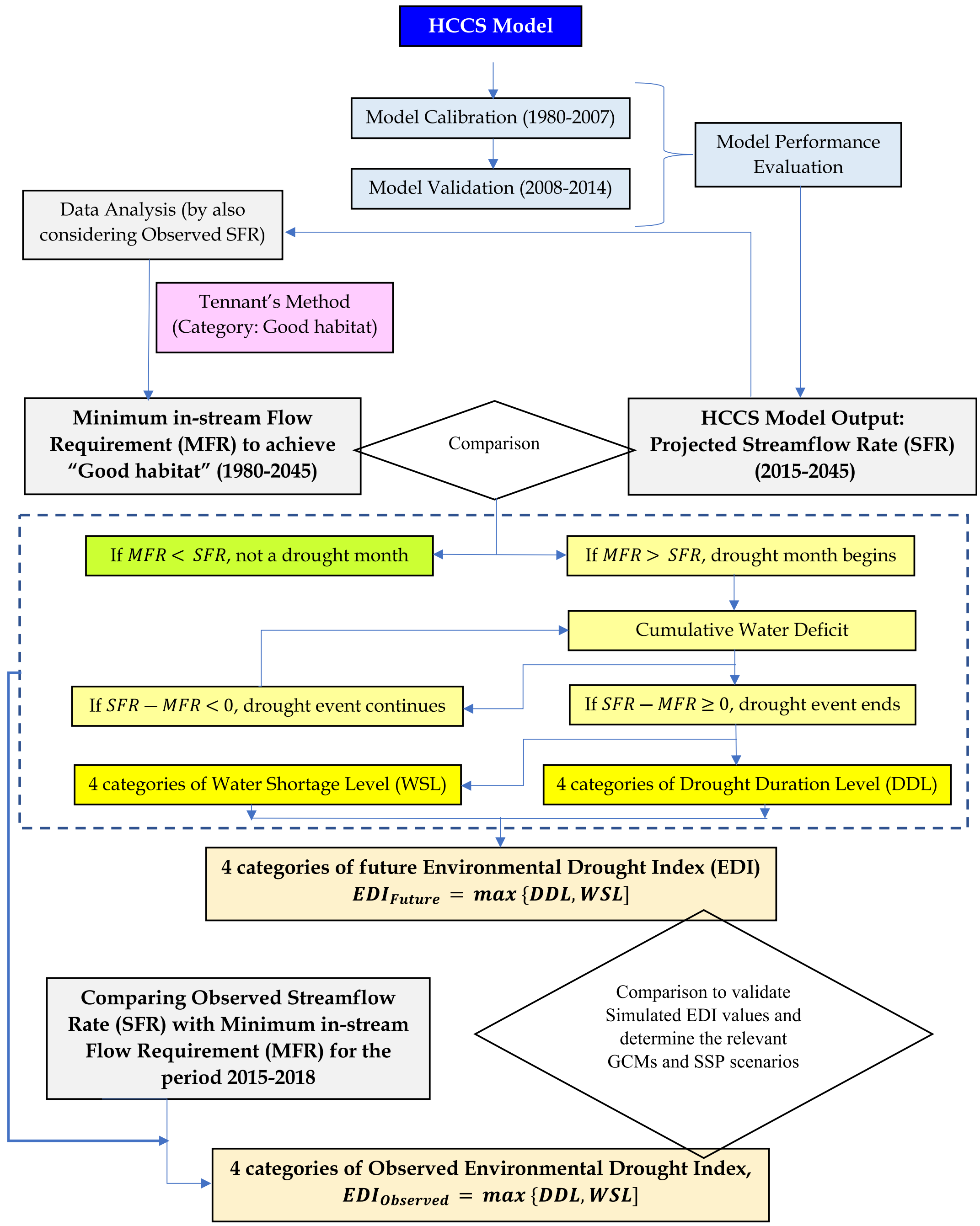

Fig. 1. Methodological flowchart for the development of the heuristic method and the Environmental Drought Index (EDI).

environmental drought. This DDL calculation constitutes one of the two primary functions of the EDI. This study establishes a framework for DDL classification by defining four distinct categories. A DDL value of 1, 2, or 3 signifies a drought event occurring at the quarterly, semi-annual, or annual scales, respectively. More specifically, a DDL value of 1 represents a drought event lasting 1 to 3 months, while a value of 2 corresponds to a duration of 4 to 6 months. Similarly, a DDL value of 3 indicates a drought event lasting 7 to 12 months, encompassing an entire year. Notably, a DDL value 4 designates a drought event persisting for longer than a year.

Second, identifying the Water Shortage Level (WSL) was a pivotal component of the EDI and constituted its second function. WSL was determined by isolating the most significant water deficit value observed during the DDL. To calculate the WSL, the absolute value of the Largest Water Deficit (LWD) during the DDL was divided by the maximum value of MFR within the same DDL, as depicted in Eqn (3). It should be noted that the Abs() function represents the absolute value calculation. In this context, the LWD was computed as the absolute difference between the SFR and MFR. As per the DDL calculation, a negative difference between SFR and MFR signifies a water deficit condition. To determine the LWD, the study identified the maximum absolute water deficit value within the DDL period, designating it as the LWD. The resulting WSL value was then classified into one of four categories. If the calculated percentage value was less than 40, the WSL was assigned a value of 1. Similarly, a percentage value between 40 and 60 led to a WSL of 2, while a value between 60 and 80 corresponded to a WSL of 3. In cases where the percentage value exceeded 80, the WSL was designated as 4.

$$WSL(in\,\%) = \frac{Abs(LWD)}{max(MFR)} \times 100 \tag{3}$$

The EDI value was derived by integrating the DDL and WSL impacts to assess each environmental drought event. Similar to the classification of DDL and WSL, the EDI in this study is also categorized into four distinct levels: slight (EDI-1), moderate (EDI-2), severe (EDI-3), and extreme (EDI-4) events of environmental drought. Determining the EDI value involves comparing the values of DDL and WSL and selecting the maximum value, as indicated in Eqn (4).

$$EDI = max\{DDL, WSL\} \tag{4}$$

Therefore, if the DDL and WSL values are 3 and 4, respectively, the resulting EDI value will be 4, signifying an extreme environmental drought event. Besides, EDI-0 represents a non-drought condition, indicating that the assessed region is not currently experiencing drought. By serving as a baseline for comparison, EDI-0 allows for distinguishing between drought and non-drought conditions, facilitating the assessment of drought severity, frequency, and percentage contribution to the total identified drought events.

Fig. 2 summarises the ranges of different EDI values based on DDL and WSL values. Since this approach ensures that the EDI captures the combined effects of the duration of the drought event (DDL) and the severity of water shortage (WSL), historical and future drought analyses can be conducted based on the proposed heuristic method and the EDI. It is crucial to emphasize that specific indicators, such as the MFR, can exhibit variations depending on land use and land cover dynamics, catchment geomorphology, scale, and even specific climate-related events within a region. Consequently, it is essential to recognize that the proposed method and index are region-dependent. It underscores the importance of recalibrating and customizing the indicators to suit different regions' specific characteristics and requirements, ultimately enabling more precise and contextually relevant analyses and assessments.

2.4. EDI validation

To ensure the reliability and robustness of the EDI, the method and index development, as described in Section 2.3, were repeated with a slight modification, as shown in Fig. 1. Instead of comparing the MFR with the simulated SFR (or future SFR), the study focused on comparing the MFR with the observed SFR. As the HCCS model had a validation period from 2008 to 2014, it provided confidence in the reliability of the generated future SFR magnitudes from 2015 to 2045. However, it became apparent that the EDI developed based on future SFR also required validation against observed SFR. The EDI values obtained from 1980 to 2014 represented the observed EDI, while the EDI values obtained from 2015 to 2045 represented the simulated or future EDI. As mentioned in Section 3.2, SFR data for 2015 to 2018 were available. This period was utilized to obtain observed EDI values for 2015 to 2018, in addition to the already available future EDI values for the FP-1 spanning 2015 to 2022. Subsequently, the observed EDI values were compared with the future EDI values extracted from FP-1 from 2015 to 2018. This comparison involved assessing the performance of six General Circulation Models (GCMs) based on two Shared Socioeconomic Pathways (SSPs) (SSP245 and SSP585). By incorporating this step into the methodology, this investigation was able to re-validate the applicability of the EDI. Additionally, it facilitated the identification of the GCM that most closely coordinated the observed EDI for the Jaraikela catchment. This information allows the findings obtained for FP-2 from this particular GCM to be considered a reliable benchmark when formulating watershed management and water resources development initiatives in the study site.

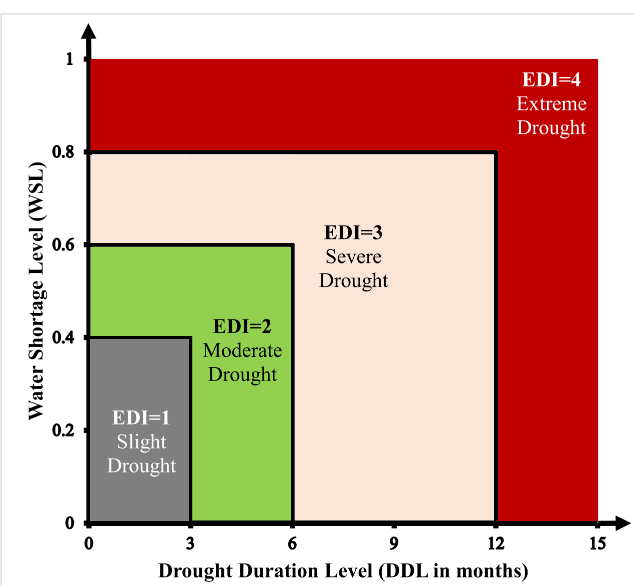

Fig. 2. Categorization of various EDI values based on different levels of drought duration (DDL) and water shortage (WSL), outlining their respective definitions and ranges [developed after Shi et al. (2018)].

3. Study site and research datasets

3.1. Study site: Jaraikela catchment

Jaraikela is a catchment of the Koel River, one of the two tributaries of the Brahmani River (the other is Sankh River), that rises near the Palamu Tiger Reserve in Jharkhand. Jaraikela represents one of the four sub-basins within the expansive Brahmani River basin, bordered by the Mahanadi River basin to the right and the Baitarani River basin to the left. This basin spans the Indian states of Chhattisgarh, Jharkhand, and Odisha, with Jharkhand alone encompassing 39.2% of the total area. The Jaraikela catchment extends between latitudes 21°50′N to 23° 36′N and longitudes 84° 29′E to 85° 49′E, covering approximately 10,637 km^2 of drainage area (refer to Fig. 3; the area is GIS-based calculated). The topography of the catchment primarily comprises flat and undulating terrains characterized by dense forests and cultivated lands. Elevation within the catchment varies from 198 m at the Jaraikela gauging site to 1,088 m in the upper (hilly) regions. The catchment area predominantly covers districts such as Lohardagga, Gumla, Ranchi, and Paschim Singhbhum in Jharkhand and parts of the Sundergarh district in Odisha. The region experiences a sub-humid tropical climate, with summer temperatures reaching as high as 47°C and winter temperatures dropping to 4°C. The average annual rainfall ranges from ~1,000 mm to ~1,300 mm, with ~80% occurring during the southwest monsoon season (June to September). The Brahmani River basin is a crucial water source for numerous towns, industries, and agricultural activities.

The Jaraikela catchment heavily relies on rainfed agriculture, but irrigation plays a significant role, particularly in the lower plains. Notably, ~80% of the catchment's water is used for irrigation. However, rapid economic development and population growth in the region have raised concerns regarding the availability of adequate irrigation water to sustain these activities. This highlights the need for comprehensive assessment and management of water resources in the catchment. Sinha et al. (2020) indicated that the Jaraikela station within the catchment experiences the highest climatic variability in India. Maximum temperature, relative humidity, and wind speed significantly influence the hydrological system. Understanding the climatic drivers and their impact on the catchment's water availability thus becomes crucial for evaluating and managing drought events in the Jaraikela catchment. Vandana et al. (2019) identified the Brahmani River basin as susceptible to temporal variations in streamflow. Their simulation results suggest a

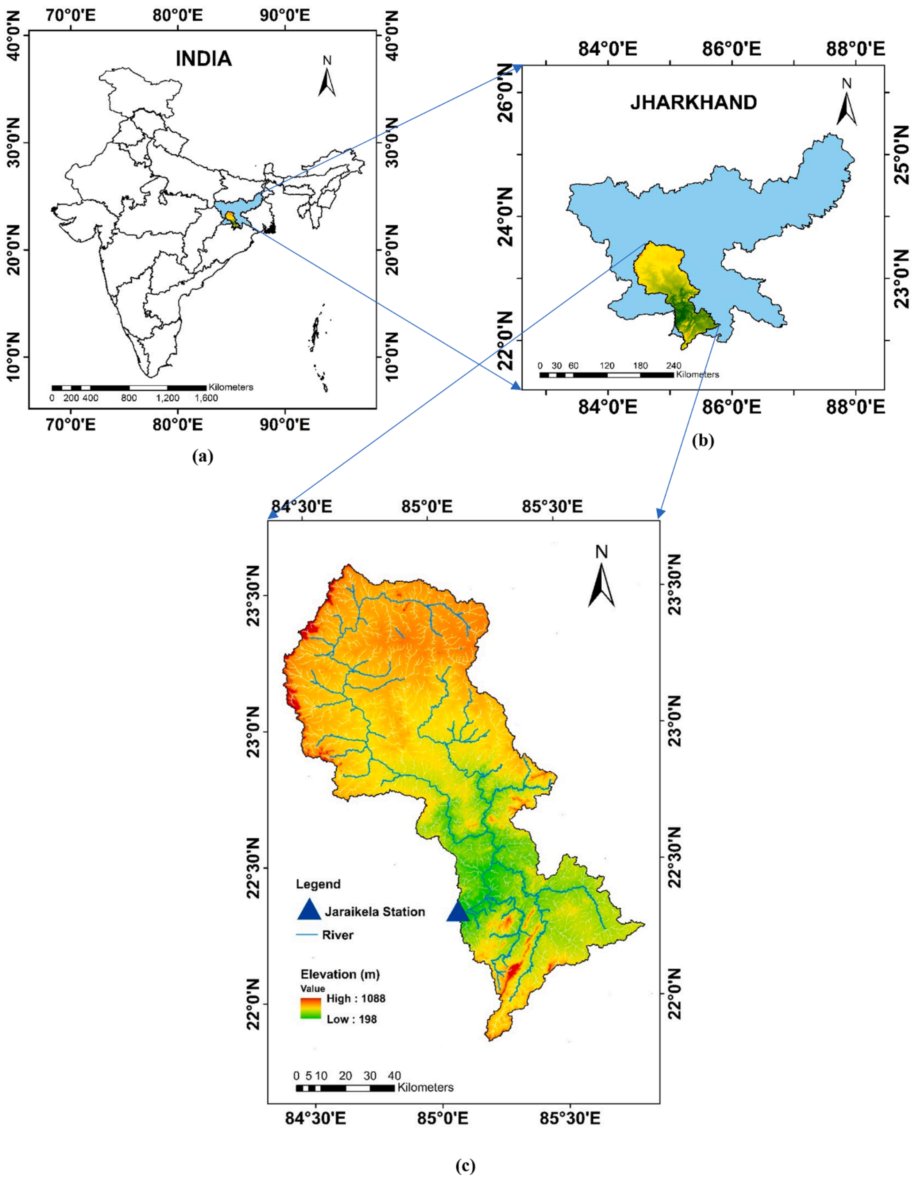

Fig. 3. Location of the study site, Jaraikela (c) [insets showing the location in Jharkhand state (b) and India (a)].

decrease in streamflow during winter, indicating the potential for recurring drought-type situations during non-monsoonal seasons. Additionally, their findings highlight an increase in flood flows and a reduction in low flows under future climate change scenarios. These insights emphasize the need to assess and monitor drought events and their impact on water resources in the catchment. Swain et al. (2020) provided evidence indicating that the Brahmani River basin is considered a high-risk zone for water scarcity, with a persistent decline in water availability. All these findings align with earlier studies (Islam et al., 2012; Amrit et al., 2018; Swain et al., 2021) that have consistently reported deteriorating water balance and water availability issues specifically for the Jaraikela catchment and broadly for Brahmani River basin. Given the challenges of water use, climatic variability, streamflow changes, and declining water availability in the Brahmani River basin, selecting the Jaraikela catchment as the study site for evaluating the novel EDI is crucial. This choice allows for an in-depth understanding of the complex dynamics of environmental drought events, their severity, and their ecological impacts.

3.2. Research datasets

To run the HCCS model, comprehensive data on streamflow, solar declination, precipitation, and temperature (mean, maximum, and minimum) at a daily resolution are essential. Daily observed SFR data spanning the period from 1980 to 2018 were obtained from the India Water Resources Information System (India-WRIS) database [India-

Table 2
Characteristics of observed Streamflow Rate (SFR) at Jaraikela catchment.

Particulars	Daily scale datasets	Monthly scale datasets
Maximum Level (meters or m)	194.630 (24 Sep 2011)	194.630 (Sep 2011)
Minimum Level (m)	186.040 (24 May 2013)	186.040 (May 2013)
Mean Level (m)	187.332	187.312
Maximum Discharge (cubic meters per second or cumecs)	12539.000 (06 Aug 1997)	12539.000 (Aug 1997)
Minimum Discharge (cumecs)	0.000 (21 Jul 2014)	0.000 (Aug 2014)
Mean Discharge (cumecs)	135.728	132.424

WRIS: https://indiawris.gov.in/wris/#/riverBasins, accessed November 2023]. Table 2 provides detailed information regarding the observed SFR, including its temporal coverage and any relevant metadata. The estimation of solar declination for the catchment followed the procedure outlined by Bhagwat and Maity (2014). It should be stressed that this study began with the use of daily observed datasets for running the HCCS model. After this initial stage, the simulated daily streamflow data, which had been obtained from the HCCS model, was processed to create aggregated monthly datasets. Table 3 further details the spatial and temporal resolution of the data utilized in this study, while further details regarding the datasets utilized in the HCCS model are presented in subsequent paragraphs.

The historical and projected hydrometeorological data for this study, encompassing precipitation, maximum temperature, minimum temperature, and mean temperature, were obtained from the NEX-GDDP-CMIP6 dataset. This dataset comprises global downscaled climate scenarios derived from the Coupled Model Intercomparison Project Phase 6 (CMIP6) runs, conducted to support the Sixth Assessment Report of the Intergovernmental Panel on Climate Change (IPCC AR6). The NEX-GDDP-CMIP6 dataset offers high-resolution and bias-corrected climate change projections well-suited for evaluating climate change impacts on processes sensitive to fine-scale climate gradients and local topographic effects, which are particularly relevant for the present study site. Detailed information about the dataset, including its derivation, can be accessed through the Earth System Grid Federation (ESGF) [NEX-GDDP-CMIP6 dataset: https://www.nccs.nasa.gov/services/data-collections/land-based-products/nex-gddp-cmip6, accessed November 2023].

Three GCMs participating in CMIP-6 were selected for this study, encompassing two emission scenarios; thus, the study employed six projected datasets (3 GCMs × 2 emission scenarios), as outlined in Table 3. These GCMs (GCM1: EC-Earth3, GCM2: MPI-ESM1-2-HR, and GCM3: MRI-ESM2-0) were selected, given that they are well-established, widely used, and have demonstrated skill in capturing relevant climatic processes in various hydroclimatological studies in India (Anil et al., 2021; Di Virgilio et al., 2022; Iqbal et al., 2021; Shetty et al., 2023; Singh, 2023). The utilization of three GCMs in this study was deemed sufficient for capturing month-wise alterations of climate projections and events of environmental drought, providing valuable insights into the dynamics of drought events in the study sites. While incorporating a larger number of GCMs could have provided additional data, the chosen number was considered adequate for achieving reasonable findings within the scope of the research. The data are sourced from two of the four 'Tier 1′ Greenhouse Gas (GHG) emissions scenarios: Shared Socio-economic Pathways. This study considered SSP245, a medium–low emissions scenario, and SSP585, a high emissions scenario. SSP245 and SSP585 are among the most widely used and well-documented scenarios within the SSP framework. Moreover, the decision to focus on SSP245 and SSP585 for this research was driven by their representation of distinct alternative futures regarding social development and GHG emissions. SSP245 corresponds to a moderate socio-economic development path (SSP2) coupled with a medium–low radiation forcing, with the radiative forcing peaking at 4.5 W/m^2 by 2100. On the other hand, SSP585 represents a high energy-intensive socio-economic development path (SSP5) characterized by strong radiative forcing, peaking at 8.5 W/m^2 by 2100. These two SSPs cover a range of plausible scenarios and provide valuable insights into different trajectories of socio-economic development and their associated GHG emissions (Ma et al., 2022; Reid et al., 2021; Yang et al., 2021; Zeydalinejad & Dehghani, 2023).

The monthly streamflow data, essential for analyzing drought events, was simulated using the HCCS model. To facilitate the study, the Jaraikela catchment was delineated, and an elevation map was created using the Shuttle Radar Topography Mission (SRTM) Digital Elevation Model (DEM) with a resolution of 30 m. This process was carried out using ArcGIS in a Geographic Information System (GIS) environment. Fig. 3 illustrates the resulting elevation map, showcasing the topographic features of the Jaraikela catchment. The SRTM DEM data was sourced from the United States Geological Survey (USGS) Earth Explorer platform [SRTM DEM data: https://earthexplorer.usgs.gov/, accessed November 2023].

4. Results

4.1. HCCS model output

Fig. 4 presents the evaluation of the HCCS model by comparing the observed and simulated values of SFR. The comparisons are depicted through time series plots on the left and scatter plots on the right. The visual analysis reveals that the model accurately captured both the direction (above or below the normal) and the magnitude of SFR. Additionally, the model demonstrates reasonable accuracy in capturing the peak values of SFR compared to the observed data. The visual interpretation thus strengthens the confidence in the reliability and effectiveness of the simulated SFR values generated by the HCCS model. While statistically also, the HCCS model demonstrated its accuracy in simulating the observed SFR data. Through rigorous assessment during the calibration period (1980–2014), the model achieved high coefficients of determination (R^2) of 0.932, 0.934, and 0.935 for GCM1, GCM2, and GCM3, respectively (refer to Fig. S2). The model validation for the period of 2008–2014 further confirmed its reliability, with R^2 values of 0.854, 0.859, and 0.865 for GCM1, GCM2, and GCM3, respectively (see Fig. 4 for details). These strong R^2 values indicate a high degree of agreement between the simulated streamflow and the observed streamflow data during the calibration and validation periods. Additionally, the HCCS model's performance indicates its ability to provide reliable streamflow projections for the Jaraikela catchment in the face of changing climate conditions. Besides, during the calibration phase, the HCCS model yielded substantial Nash-Sutcliffe Efficiency (NSE) values of 0.859, 0.862, and 0.861 for GCM1, GCM2, and GCM3, respectively. The rigorous validation of the model's capabilities consistently affirmed its robustness, as evidenced by NSE values of 0.754, 0.764, and 0.786 for GCM1, GCM2, and GCM3, respectively. These NSE values serve as strong indicators of the model's ability to accurately replicate observed streamflow dynamics, thus underlining its reliability in simulating hydrological processes. Altogether, these findings validate the reliability of the HCCS model in accurately representing the hydrological processes, thereby enabling its effective utilization for generating simulated SFR for FP-1 and FP-2.

Table 3
Summary of six selected datasets (3 CMIP6-GCM models × 2 emission scenarios).

Climate Model	Emission scenarios	Radioactive forcing by 2100	An update on which RCP?	Characteristics	Data resolution	Period
3 IPCC GCMs: EC-Earth3 MPI-ESM1-2-HRMRI-ESM2-0	SSP245	4.5 W/m^2	RCP4.5	Middle of the road (intermediate challenges)	• Latitude: 0.25 degrees (25 km) • Longitude: 0.25 degrees (25 km) • Temporal: daily (converted to monthly)	1980–2045
	SSP585	8.5 W/m^2	RCP8.5	Taking the highway (mitigation challenges dominate)		

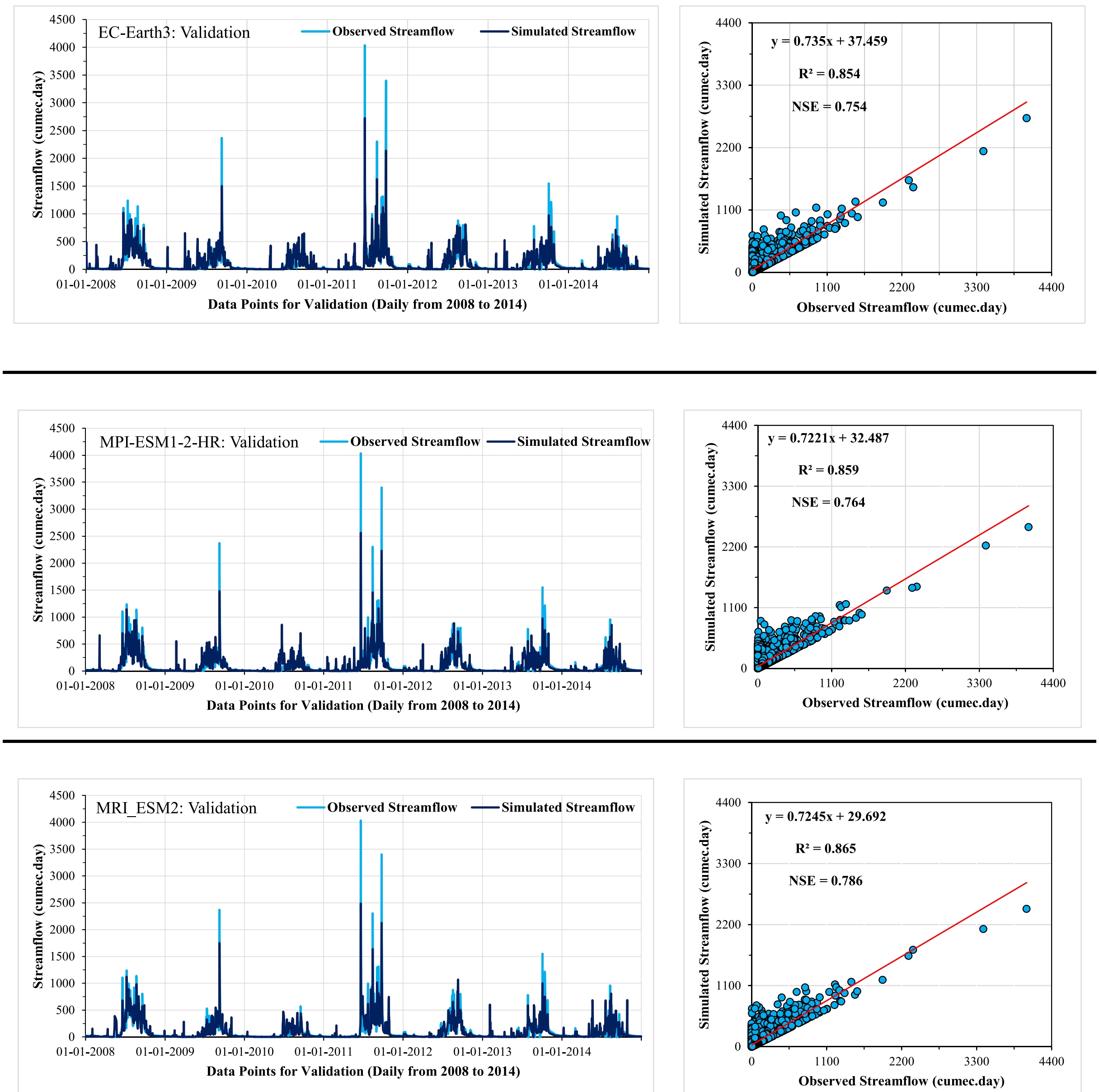

Fig. 4. Comparison between observed and simulated daily streamflow (obtained using the HCCS model) for the Jaraikela catchment during the validation period (2008–2014) for the three General Circulation Models (GCMs viz., EC-Earth3, MPI-ESM1-2-HR, and MRI-ESM2) output ensembles using time series plots (left-side) and scatter plots (right-side) [In the scatter plots, the solid black line shows the 45° line (1:1; line of perfect simulation), and the other line shows the best-fit line for the scatter points].

4.2. Analysis of flow hydrograph

Table 1 presents the results of applying Tennant's method to determine the MFR for each month based on the entire base period (1980–2014). During the LFS, the average monthly MFR was found to be 27.41 cumecs (m^3/s); during the HFS (excluding August), it was 54.83 cumecs. However, for August, which accounted for additional flushing flows, the average monthly MFR increased to 63.67 cumecs. Considering the flow hydrograph, as shown in Fig 5, analysis of the southwest monsoon season (June to September in India) revealed that the observed SFR was ~7 times higher than the calculated MFR, indicating the absence of environmental drought events in the Jaraikela catchment during the monsoonal months (when the entire 35-year period considered together). This pattern remained consistent during the post-monsoon season (October to December), with the observed SFR remaining around 2–3 times higher than the calculated MFR for October and November and comparable for December. However, during the winter season (January and February) and the summer or pre-monsoon season (March to May), the observed SFR was significantly lower than the calculated MFR, ranging from 0.7 to 0.5 times for the winter season and 0.3 to 0.2 times for the summer season. This noteworthy observation highlighted the importance of determining the MFR on a monthly basis and comparing it with the SFR to generate flow hydrographs for the observed period (Fig. S3), as well as for FP-1 (Fig. S4) and FP-2 (Fig. S5). A consistent inference observed from these flow hydrographs was that during the monsoon and post-monsoon seasons, both the observed and simulated SFR values were generally higher compared to the calculated MFR values, for both the observed and future periods. On the other hand, non-monsoonal seasons showed the opposite results, with lower SFR values compared to the calculated MFR values. It thus became crucial to quantify the magnitude of water shortage and drought duration by comparing MFR values with the observed SFR (detailed in

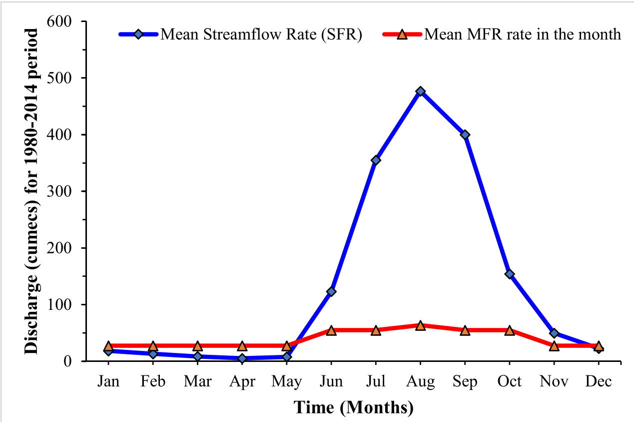

Fig. 5. Demonstration of observed monthly variation of Streamflow Rate (SFR) against Minimum in-stream Flow Requirement (MFR) for Jaraikela catchment using Tennant's method [Note: Here, each month is representative of the mean discharge over the period 1980–2014 (35 years)].

Section 4.3) and simulated SFR for the three GCMs under two future emission scenarios (detailed in Sections 4.4 and 4.6). Additionally, the severity of environmental drought is required to be assessed by employing the EDI so as to quantify the occurrence of the environmental drought on a monthly basis during the observed and future periods (detailed in the following sections and discussed in Section 5.2).

4.3. Historical environmental drought analysis

Fig. 6a shows the plot between the magnitude difference of SFR and MFR for the observed period (1980–2014) for the Jaraikela catchment and different EDI values. Fig. 6b displays the number of environmental drought events based on different EDI values, drought period lengths, and different levels of water shortage. A total of 38 environmental drought events were identified between 1980 and 2014. These events were observed every year, highlighting the occurrence of environmental droughts during non-monsoonal seasons. Moreover, this also indicated the recurring challenge of meeting the environmental flow requirements to maintain a "Good Habitat" condition in the catchment. Among the recorded events, severe droughts (EDI-3) were the most frequent, with 17 occurrences, followed closely by moderate droughts (EDI-2), with 16 events. This suggests that the catchment frequently encountered significant deficits in water availability, impacting its ecological health. The analysis of the EDI components revealed that DDL had a greater influence on the index than WSL, as the number of EDI events closely aligned with the number of DDL events. This indicates that the length of time over which the catchment experienced water deficits significantly affected the degree of environmental droughts. The study did not observe any extreme environmental drought events (EDI-4), where droughts extended for over 12 months (DDL-4) or experienced water shortages exceeding 80 % (WSL-4). This implies that the catchment did not face exceptionally severe and prolonged drought conditions during the study period. Semi-annual and annual drought events (DDl-2 and DDL-3, respectively) were the most prevalent, with water shortages of less than 40 % (WSL-1) being the most frequently observed scenario (30 events), followed by shortages of 40–60 % (WSL-2; 7 events). Overall, these inferences provide valuable insights into the environmental drought dynamics in the Jaraikela catchment, highlighting the need to further investigate the EDI and its components, DDL and WSL's impacts, in near and far future periods across the Jaraikela catchment.

4.4. Future environmental drought analysis: FP-1 (2015–2022)

Fig. 7 shows the plot between the magnitude difference of SFR and MFR and different EDI values for GCM1, 2, and 3 under SSP245 and SSP585 for FP-1. In Fig. 8, the numbers of environmental drought events are presented based on different EDI values, drought period lengths (DDL), and levels of water shortage (WSL) for the same GCMs, scenarios, and study period as in Fig. 7. Under the SSP245 scenario (Figs. 7 and 8; left), GCM1 identified 15 environmental drought events, while both GCM2 and GCM3 identified 17 events. In contrast to the findings from the observed period, the WSL component was found to have a more substantial influence on the EDI values, as EDI and WSL values were closely aligned for all three GCMs. The most prevalent environmental drought events recorded by all GCMs were moderate droughts (EDI-2) during FP-1, with the corresponding dominant WSL falling between 40% and 60% (WSL-2). Additionally, quarterly drought (DDL-1) events were most prominent among the DDL categories across the GCMs. Interestingly, GCM1 and GCM2 did not show any occurrence of extreme drought events, with EDI-4, DDL-4, and WSL-4 values being zero. However, GCM3 exhibited two extreme drought events, where WSL-4 had a value of 2 and dominated over DDL. These findings provide valuable insights into the projection of environmental drought events. The strong alignment between EDI and WSL values indicates the significance of water shortage in shaping future environmental drought conditions. Additionally, the prominence of moderate (EDI-2) and quarterly drought (DDL-1) events highlights their potential impact on the catchment's ecosystem and water resources. However, further research and validation are essential to enhance the understanding and prediction of environmental drought events under different climate scenarios. To achieve this, the SSP585 scenario was also incorporated to assess the potential alterations in the severity of environmental drought events using the same GCMs.

Under the SSP585 scenario (Figs. 7 and 8; right), GCM1 and GCM3 identified 15 environmental drought events, while GCM2 identified 13 events, all nearly consistent with the number of drought events identified under SSP245. Besides, compared to SSP245, a significant shift was observed toward an increased number of severe drought (EDI-3) events for all GCMs under SSP585. Despite this shift, similar to SSP245, the WSL component remained a strong influencer of the EDI values, with EDI and WSL values aligning across all three GCMs. Furthermore, despite the increase in severe drought under SSP585, moderate droughts (EDI-2) were consistently the most prevalent environmental drought events recorded by all GCMs, with the corresponding dominant WSL ranging between 40% and 60% (WSL-2). Additionally, quarterly drought (DDL-1) events were the most prominent among the DDL categories across the GCMs, closely followed by semi-annual drought (DDL-2) events. In contrast, GCM1 and GCM3 exhibited two extreme drought (EDI-4) events, while GCM2 showed no occurrence of extreme droughts, making it an exception.

The analysis for FP-1 revealed a prevalence of moderate drought events under both future scenarios, with the WSL being the primary influencing component. This finding highlights the importance of focusing on moderate droughts (EDI-2) while devising drought management and resilience strategies in the Jaraikela catchment, given FP-1. Furthermore, the degree of water shortage remains crucial in determining the severity of environmental droughts, irrespective of the future emission scenarios considered. Notably, drought events lasting longer than 12 months (DDL-4) were absent in both scenarios. Additionally, there was a notable difference in the occurrence of slight (EDI-1) and severe drought (EDI-3) events between the two scenarios. Under SSP245, slight drought events were more frequent than severe drought events, while under SSP585, the opposite pattern was observed, with more occurrences of severe drought events compared to slight drought events. This shift indicates a potential escalation in the severity of droughts in the future, thereby demanding an analysis of the possible alterations during FP-2 (conducted in Section 4.6). Moreover, this suggests that droughts in the catchment exhibit seasonal variability, with certain periods experiencing more prolonged water deficits than others. Moreover, the findings described in this section raise a crucial question

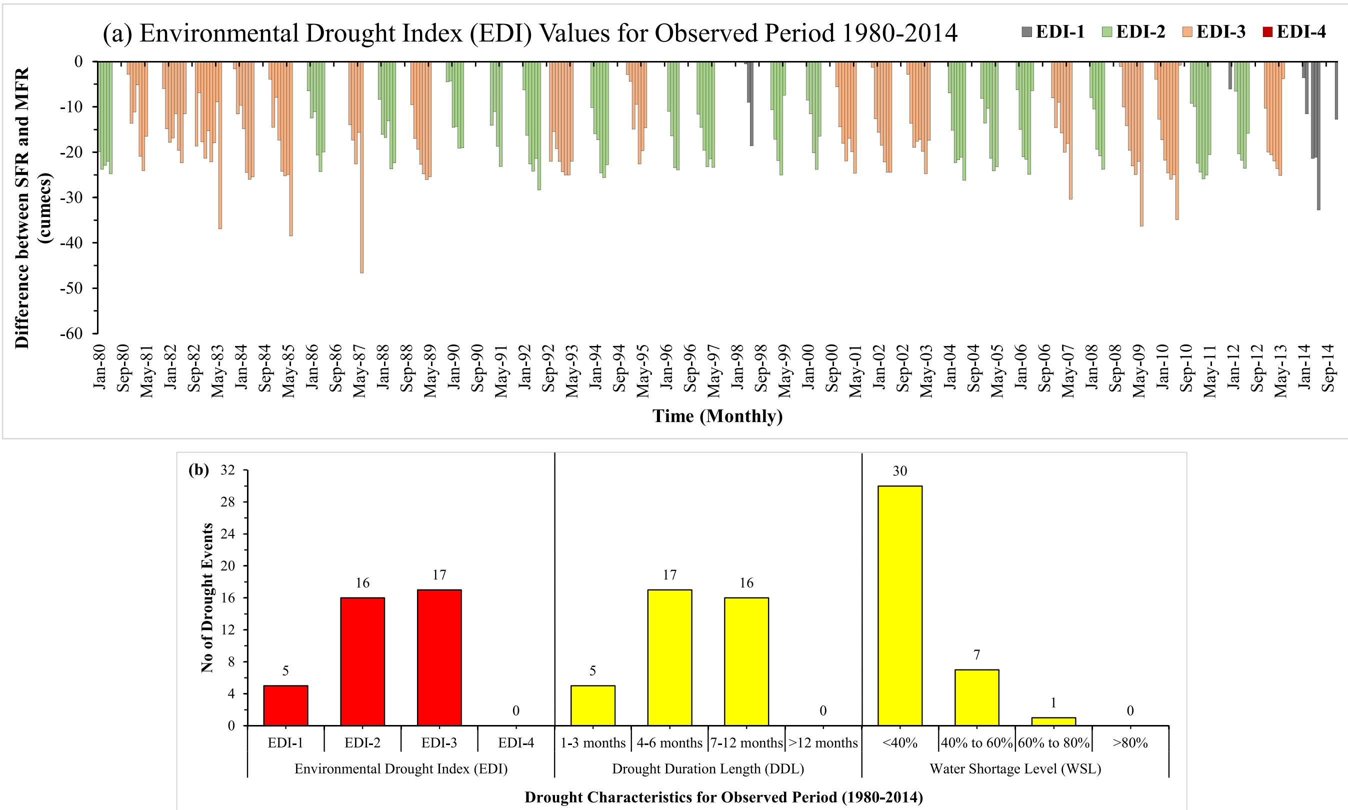

Fig. 6. (a) The magnitude difference between Streamflow Rate (SFR) and Minimum in-stream Flow Requirements (MFR) on the Y-axis (negative magnitude indicates water deficit while positive magnitude indicates water sufficiency and thus not shown) and with different EDI values (EDI-1, EDI-2, EDI-3, and EDI-4) on X-axis for the observed period (1980–2014) at Jaraikela catchment; (b) The numbers of environmental drought events with different EDI values and for different lengths of the drought period (DDL in months; 1–3, 4–6, 7–12, and > 12) and for different levels of water shortage (WSL in %; <40, 40–60, 60–80, and > 80) for the observed period (1980–2014) at Jaraikela catchment.

about which scenarios should be given more attention to better understand the degree of environmental drought events in the Jaraikela catchment. To address this, the study conducted an EDI validation (see Section 4.5) to determine the scenario and, specifically, the GCM that best represents the present actual conditions in the study area. The EDI validation step will help identify the most reliable projection for future environmental drought events (especially for FP-2), which will undoubtedly influence the current and future decision-making and adaptation strategies.

4.5. Analysis from EDI validation

Fig. S6 presents the flow hydrograph, showcasing the observed monthly variation of SFR and its comparison with MFR for the Jaraikela catchment during the observed period from 2015 to 2018. Like Fig. 6 and Figs S3 to S5, this hydrograph provides essential insights into the streamflow conditions in the catchment over these years. However, it is crucial to note that the observed data is available only until 2018, limiting the validation period to 2015–2018, and the entire 2015–2022 (FP-1) period could not be considered for validation. Moreover, for the FP-1, the study utilized the processed data from the HCCS model, namely the simulated SFR, to apply the EDI methodology. Therefore, the primary objective of this comparison, as shown in Figs. 9 and 10, was to assess the variations between the observed EDI and its components (developed using observed SFR) and the simulated EDI and its components (developed using simulated SFR).

Considering first the observed EDI, this case revealed a total of five drought events, with two classified as moderate drought (EDI-2) and the remaining three as severe drought (EDI-3) during 2015–2018. This suggests that the catchment experienced multiple episodes of environmental drought during the observed period on a yearly basis, affecting its water resources and ecosystem health. The severity of drought events was primarily influenced by the duration of the drought, as evident from the dominance of DDL in severe drought events. In contrast, moderate drought events were influenced by a combination of both WSL and DDL, indicating that shorter but more intense droughts also contributed to environmental stress. The study evaluated the EDI, DDL, and WSL values for the three GCMs under SSP245 and SSP585 scenarios to gain further insights and compare these findings (see Fig. 10).

Considering the simulated EDI under the SSP245 scenario, GCM1 and GCM3 displayed eight drought events each, while GCM2 exhibited ten events, in contrast to the observed five events. These results suggest that the GCMs' projections did not precisely capture the EDI values under SSP245, as they tended to overestimate the number of moderate drought events and generally underestimate the occurrences of severe drought events. Similar discrepancies were observed in assessing DDL and WSL components. For instance, GCM1, GCM2, and GCM3 identified six, six, and four moderate drought (EDI-2) events, respectively, in contrast to the observed two events. Similarly, the occurrences of severe drought (EDI-3) events were projected as one, four, and two by GCM1, GCM2, and GCM3, respectively, whereas the observed data recorded three events. These disparities in the simulated EDI, DDL and WSL levels for each GCM compared to the observed data indicate the challenges in accurately predicting environmental drought events for the SSP245 scenario. The comparison of the observed data with the SSP585 scenario becomes necessary to gain a comprehensive understanding of potential changes in environmental droughts.

Under the SSP585 scenario, GCM1 and GCM2 exhibited five drought events, matching the observed data. However, GCM3 displayed eight

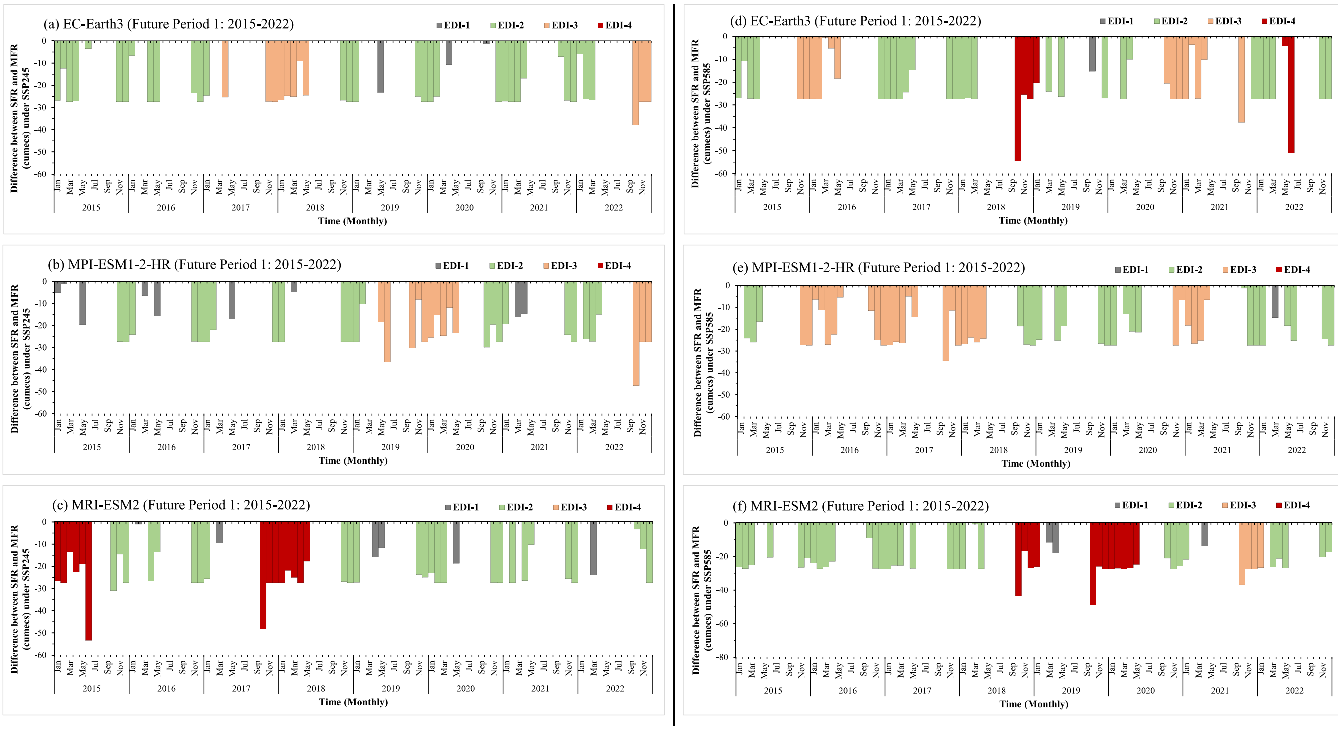

Fig. 7. Magnitude difference between Streamflow Rate (SFR) and Minimum in-stream Flow Requirements (MFR) on Y-axis (negative magnitude indicates water deficit while positive magnitude indicates water sufficiency and thus not shown) and with different EDI values (EDI-1, EDI-2, EDI-3, and EDI-4) on X-axis for the three General Circulation Models (GCMs viz., EC-Earth3, MPI-ESM1-2-HR, and MRI-ESM2) under the two future scenarios [SSP245 (left-side; a to c) and SSP585 (right-side; d to f)] for the first future period (2015–2022).

drought events, deviating from the observed five. A comparison between GCM1 and GCM2 revealed differences in the number of identified different types of drought events. For instance, GCM1 exhibited one extreme drought (EDI-4) event absent in GCM2. Nonetheless, GCM2 precisely replicated the number of environmental drought events, with the DDL and WSL aligning closely with the observed time series. The corresponding DDL and WSL values for GCM2 matched the observed datasets, further validating its accuracy in representing the observed conditions in the Jaraikela catchment. As a result, the study identified GCM2, known as "MPI-ESM1-2-HR," under SSP585 as the most accurate representation of the present observed environmental drought conditions in the study area.

GCM2's reliable predictions of environmental drought events under SSP585 can play a crucial role in informing robust decisions to address the challenges posed by future drought occurrences. With this validation, utilizing GCM2's projections to determine and prepare for environmental drought events during FP-2 is imperative. Nevertheless, this study will not overlook the findings from other GCMs and scenarios. Considering a wide range of possible drought conditions in the future will facilitate a more comprehensive understanding of potential environmental drought impacts, thereby providing scope to tackle the uncertainties associated with environmental droughts.

4.6. Future environmental drought analysis: FP-2 (2023–2045)

Fig. S7 displays the plot representing the magnitude difference between SFR and MFR for GCM1, GCM2, and GCM3 under SSP245 and SSP585 scenarios during FP-2, with variations in different EDI values. Additionally, Fig. 11 presents the numbers of environmental drought events based on various EDI values, drought period lengths (DDL), and levels of water shortage (WSL) for the same GCMs, scenarios, and study period, as shown in Fig. S7. Under the SSP245 scenario (Figs. S7 and Fig. 11; left), the GCMs identified a range of 35 to 42 environmental drought events. In contrast to the observed period and FP-1 findings, moderate drought (EDI-2) events were strongly influenced by the 40–60% water shortage condition (WSL-2), while severe drought (EDI-4) events were influenced by a drought length of 7 to 12 months (DDL-3). This was evident from the close alignment of EDI values with WSL for moderate droughts and DDL for severe droughts. During FP-2, similar to FP-1, the most prevalent environmental drought events recorded by all GCMs were moderate droughts, with the corresponding dominant component WSL falling between 40% and 60%. Severe drought events with the corresponding dominant component DDL of the category annual drought followed this. Additionally, similar to FP-1, quarterly drought (DDL-1) events were the most prominent among the DDL categories across the GCMs during FP-2. However, unlike FP-1, all the GCMs during FP-2 exhibited extreme drought events, ranging from five for GCM3 to one for GCM2. EDI's water shortage component (rather than the length of the drought) was identified as the cause behind extreme drought events. It can be inferred that the severity of the droughts increased from FP-1 to FP-2 under SSP245; however, this inference would require identifying the percentage contribution of each drought type in the respective study period (discussed in Section 5.1). Since the EDI validation findings showcased GCM2 under SSP585 as the closest representative model, analyzing FP-2 under this scenario became imperative to determine the alterations from SSP245 to SSP585.

Under the SSP585 scenario (Figs. S7 and Fig. 11; right), the GCMs identified environmental drought events in the range of 36 to 41, nearly consistent with the number of drought events identified under SSP245. However, a notable shift was observed, indicating an increased number of severe (EDI-3) and extreme drought (EDI-4) events for all GCMs under SSP585 compared to SSP245. Similar to the findings in FP-1, the WSL component remained a strong influencer of the EDI values during FP-2 under both SSP245 and SSP585, with EDI and WSL values generally aligning across all three GCMs. Interestingly, the dominant environmental drought event during FP-2 under SSP585 was severe drought events recorded by all GCMs, with the corresponding dominant WSL ranging between 60% and 80% (WSL-3). However, quarterly drought

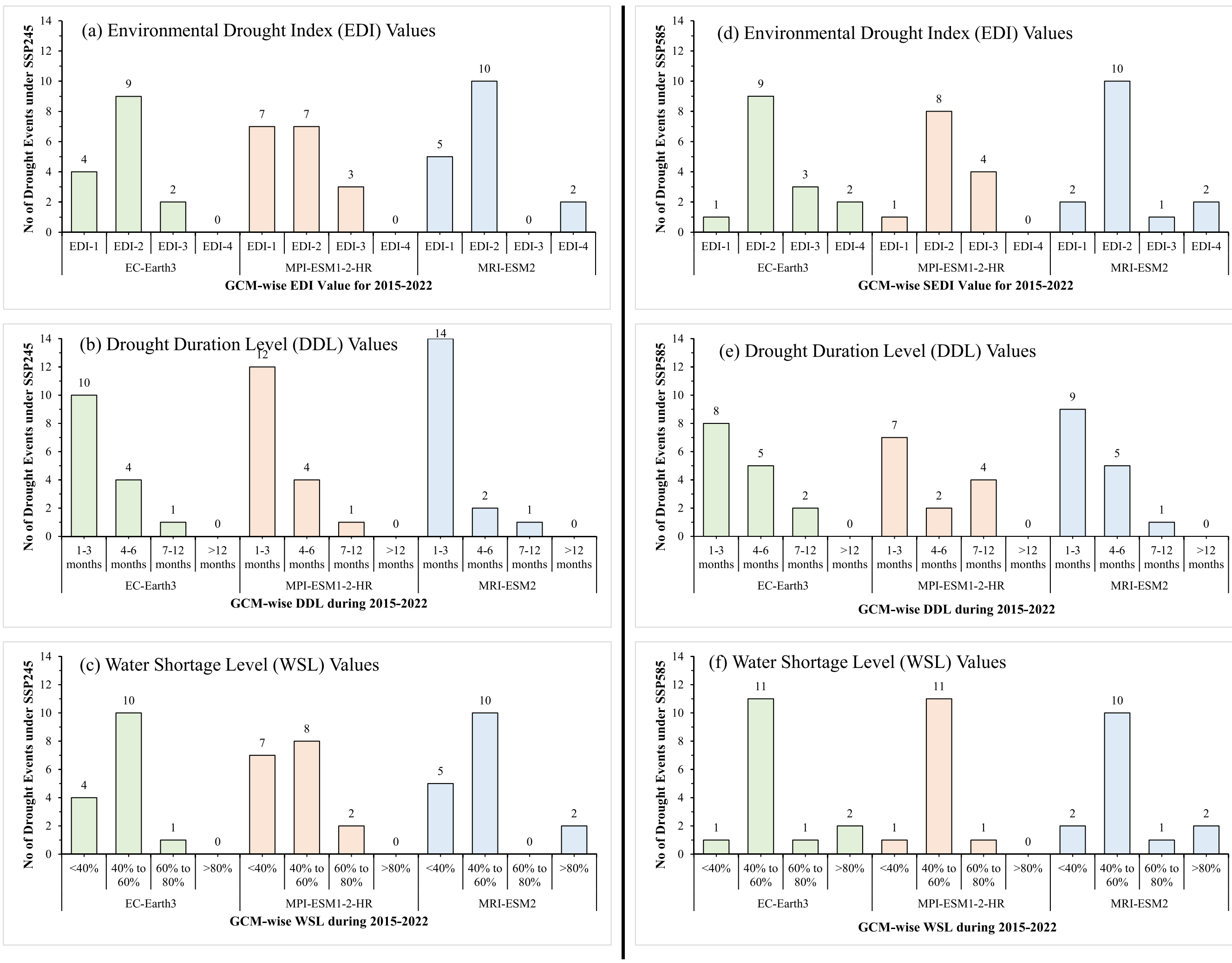

Fig. 8. The numbers of environmental drought events with different EDI values (EDI-1, EDI-2, EDI-3, and EDI-4) and for different lengths of the drought period (DDL in months; 1–3, 4–6, 7–12, and > 12) and for different levels of water shortage (WSL in %; <40, 40–60, 60–80, and > 80) for the three General Circulation Models (GCMs viz., EC-Earth3, MPI-ESM1-2-HR, and MRIESM2) under the two future scenarios [SSP245 (left-side; a to c) and SSP585 (right-side; d to f)] for the first future period (2015—2022) at Jaraikela catchment.

events were the most prominent among the DDL categories across the GCMs, closely followed by semi-annual drought (DDL-2) events, consistent with the findings for FP-1 under both scenarios. Notably, an increase in the number of extreme drought (EDI-4) events was recorded compared to SSP245, ranging from five identified by GCM1 and GCM2 to eight by GCM3. Considering the findings from GCM2 (the closest representative model) exclusively, it indicates a possibility of 29 severe drought (EDI-3) events out of the 41 identified, followed by five extreme drought (EDI-4) events and five moderate drought (EDI-2) events.

The analysis for FP-2 revealed a prevalence of moderate drought (EDI-2) events under SSP245 and severe drought (EDI-3) events under SSP585 scenarios, with the WSL being the primary influencing component. This suggested that future climatic conditions may lead to more frequent and intense droughts in the catchment. This further indicated a heightened risk of extended periods of water shortage and highlighted the need for management strategies to cope with prolonged drought conditions. To re-emphasize, the close alignment between EDI and WSL values across all three GCMs suggested that water scarcity plays a crucial role in driving environmental drought conditions in the catchment. Since the occurrence of quarterly drought (DDL-1) events remained the most prominent among the DDL categories across the GCMs, for both scenarios and FPs, shorter-term drought events may parallelly have a significant impact on the catchment's hydrological regime. Overall, the study highlights the importance of considering different emission scenarios and GCMs to understand the potential impacts of environmental drought in the Jaraikela catchment. The increase in severe (EDI-3) and extreme drought (EDI-4) events under SSP585 during FP-2 emphasizes the urgency of implementing adaptive measures and robust water resource management strategies to safeguard the catchment's water availability and ecological health in the coming decades.

5. Discussion

5.1. Analysing the change between the observed period, FP-1 and FP-2

The investigation encompassed three different study periods with varying lengths: 35 years for the observed period (1980–2014), eight years for FP-1 (2015–2022), and 23 years for FP-2 (2023–2045). Comparing the specific alterations in EDI, DDL, and WSL values between the observed and future periods (FP-1 and FP-2) required an approach that could accommodate periods of different lengths. To address this, the study developed Fig. 12, which facilitated a comparative analysis of the percentage contribution of each drought characteristic at the Jaraikela station across the mentioned study periods. In Fig. 12, the percentage of specific drought characteristics (EDI, DDL, and WSL) is represented by numbers in the sunburst plots. These percentages were calculated based

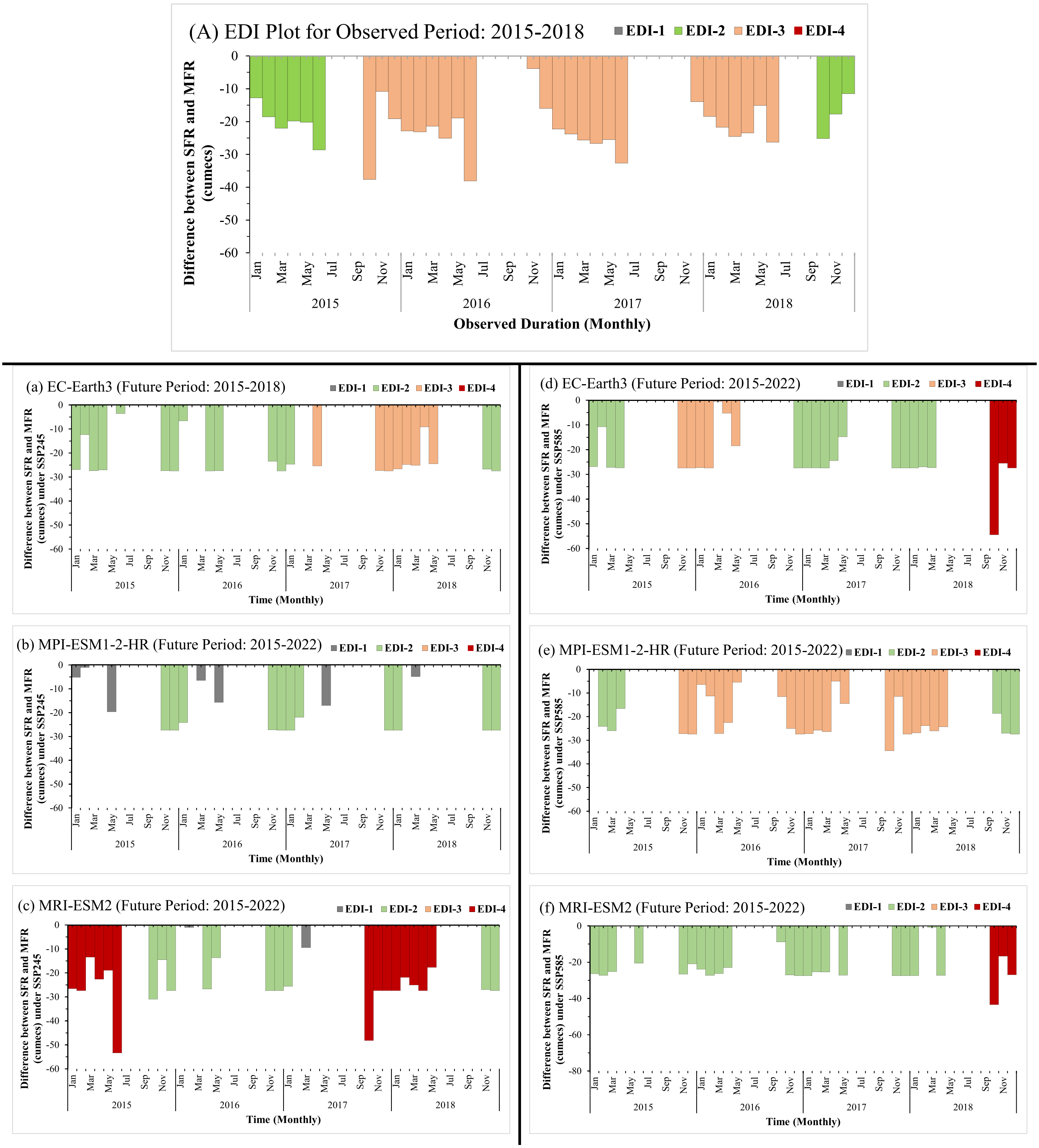

Fig. 9. The magnitude difference between Streamflow Rate (SFR) and Minimum in-stream Flow Requirements (MFR) on Y-axis (negative magnitude indicates water deficit while positive magnitude has not been shown as it indicates water sufficiency) and with different EDI values (EDI-1, EDI-2, EDI-3, and EDI-4) on X-axis for the observed period (2015–2018) at Jaraikela catchment; demonstration "A" (most-top) is for the observed discharge and is compared with simulated discharge obtained from the three GCMs for two future scenarios viz., SSP245 (left-side; a to c) and SSP585 (right-side; d to f).

on the ratio of the number of specific events (e.g., EDI-1 events) to the total number of events (sum of EDI-1, EDI-2, EDI-3, and EDI-4 events). This approach allowed to comprehensively understand the contribution of different drought characteristics and dynamics of environmental drought in the Jaraikela catchment across the observed and future study periods.

During the observed period [Fig. 12(i)], the occurrence of severe drought (EDI-3) events accounted for 45% of the cases, closely followed by moderate drought (EDI-2) events at 42%. The predominant driver for these droughts was the length of the drought duration, with 42% of the environmental droughts classified as annual droughts (DDL-3) and 45% as semi-annual droughts (DDL-2). This indicates that the duration of dry

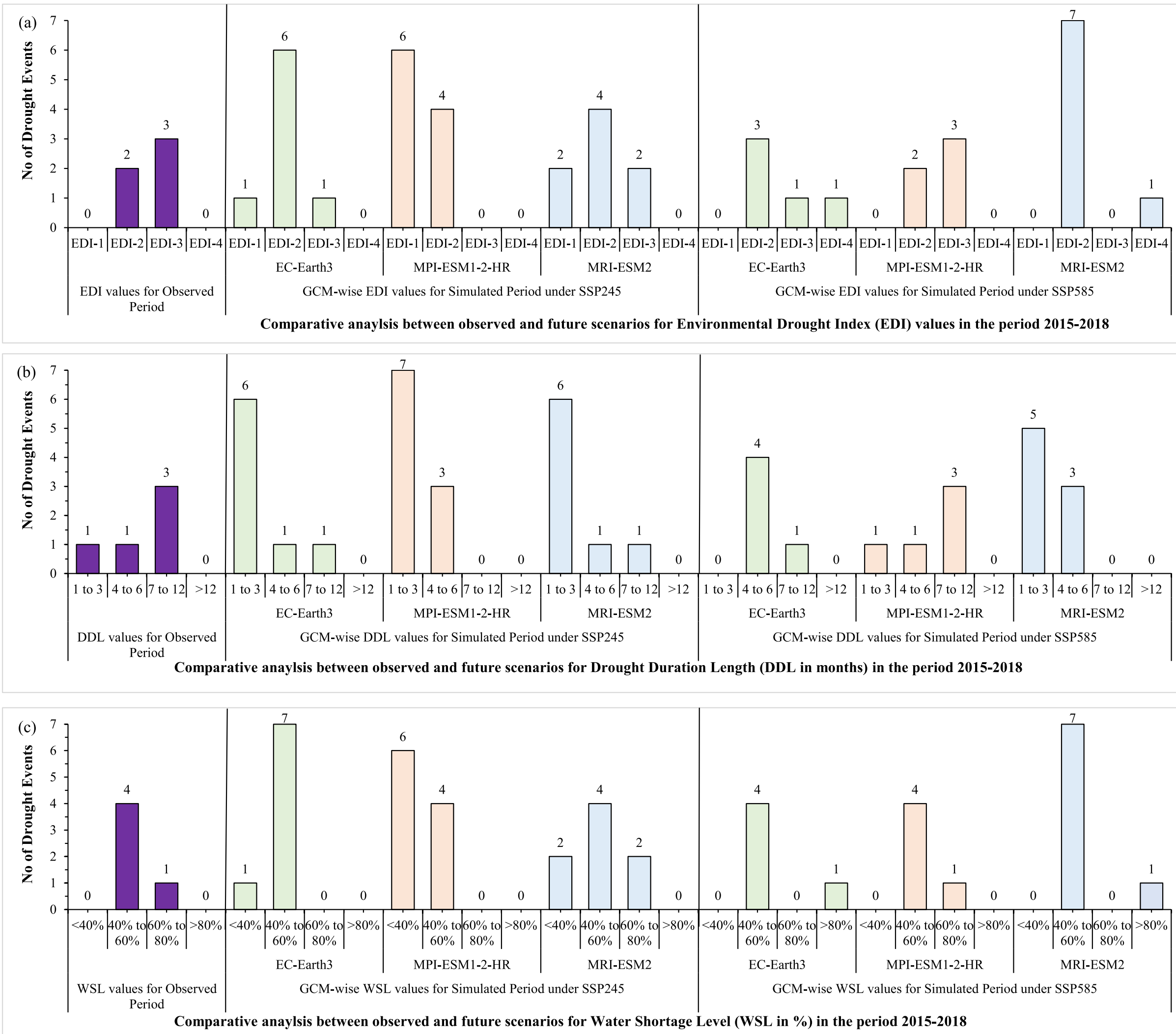

Fig. 10. Comparative analysis for the numbers of environmental drought events with different EDI values [as shown in (a)] and for different lengths of the drought (DDL) period [as shown in (b)] and for different levels of water shortage (WSL) [as shown in (c)] between the observed datasets and the three General Circulation Models (GCMs viz., EC-Earth3, MPI ESM1-2-HR, and MRI-ESM2) under the two future scenarios [SSP245 (left-side) and SSP585 (right-side)] for the period 2015–2018 at Jaraikela catchment [Note: The observed data for Jaraikela catchment is available only for the period 1980–2018 in the public domain; thus, the present study does not compare the observed findings with the entire first future period (i.e., 2015–2022) but is limited to comparing it with 2015–2018 period].

periods was a critical factor in shaping the frequency and intensity of environmental droughts in the catchment. Additionally, 79% of the environmental drought cases experienced a water shortage of less than 40 % (WSL-1), indicating that the observed environmental droughts were primarily influenced by the DDL component rather than the WSL component. The dominance of severe and moderate droughts, coupled with the influence of drought duration and water shortage level, emphasized the significance of studying and preparing for potential future drought events.

During FP-1 under SSP245 [Fig. 12(ii[a, b, c])], all three GCMs consistently identified moderate drought (EDI-2) events as the most common type, representing 60%, 41%, and 59% of the total drought events for GCM1, GCM2, and GCM3, respectively. This finding contrasted with the observations made during the 1980–2014 period. The prevailing droughts component primarily influenced the WSL droughts, particularly cases with 40% to 60% water shortage (WSL-2). Additionally, the most frequent category of the DDL component was the slight drought (EDI-1) events. While under SSP585 [Fig. 12(ii[d, e, f])], all GCMs again identified moderate drought (EDI-2) events as the most common, accounting for 60%, 62%, and 67% of total drought events for GCM1, GCM2, and GCM3, respectively. This indicated a higher percentage contribution than under SSP245. However, a notable contrast was observed in the prevalence of severe drought (EDI-3) events, which accounted for 20%, 31%, and 7%, respectively. This was in contrast to the occurrence of slight drought (EDI-1) events observed under SSP245. Moreover, another significant difference was the presence of extreme drought (EDI_4) events, particularly identified by GCM1 (13%) and GCM3 (13%). Overall, the findings presented in the above discussion align well with the results reported in Section 4.4.

During FP-2 under SSP245 [Fig. 12(iii[a, b, c])], all three GCMs consistently identified moderate drought (EDI-2) events as the most common type, representing 63%, 71%, and 50% of the total drought events for GCM1, GCM2, and GCM3, respectively. This finding contrasted with the observations made during the 1980–2014 period, where severe droughts (EDI-3) were more prevalent, and the percentage contribution of moderate drought events remained higher than the SSP245 findings for FP-1. Regarding the DDL and WSL components, the findings for FP-2 under SSP245 were similar to the SSP245 findings for FP-1. However, there was a notable increase in identifying extreme drought (EDI-4) events by all GCMs, with percentages of 6%, 2%, and 14% for GCM1, GCM2, and GCM3, respectively. This indicates a potential shift towards more extreme drought (EDI-4) events in the future

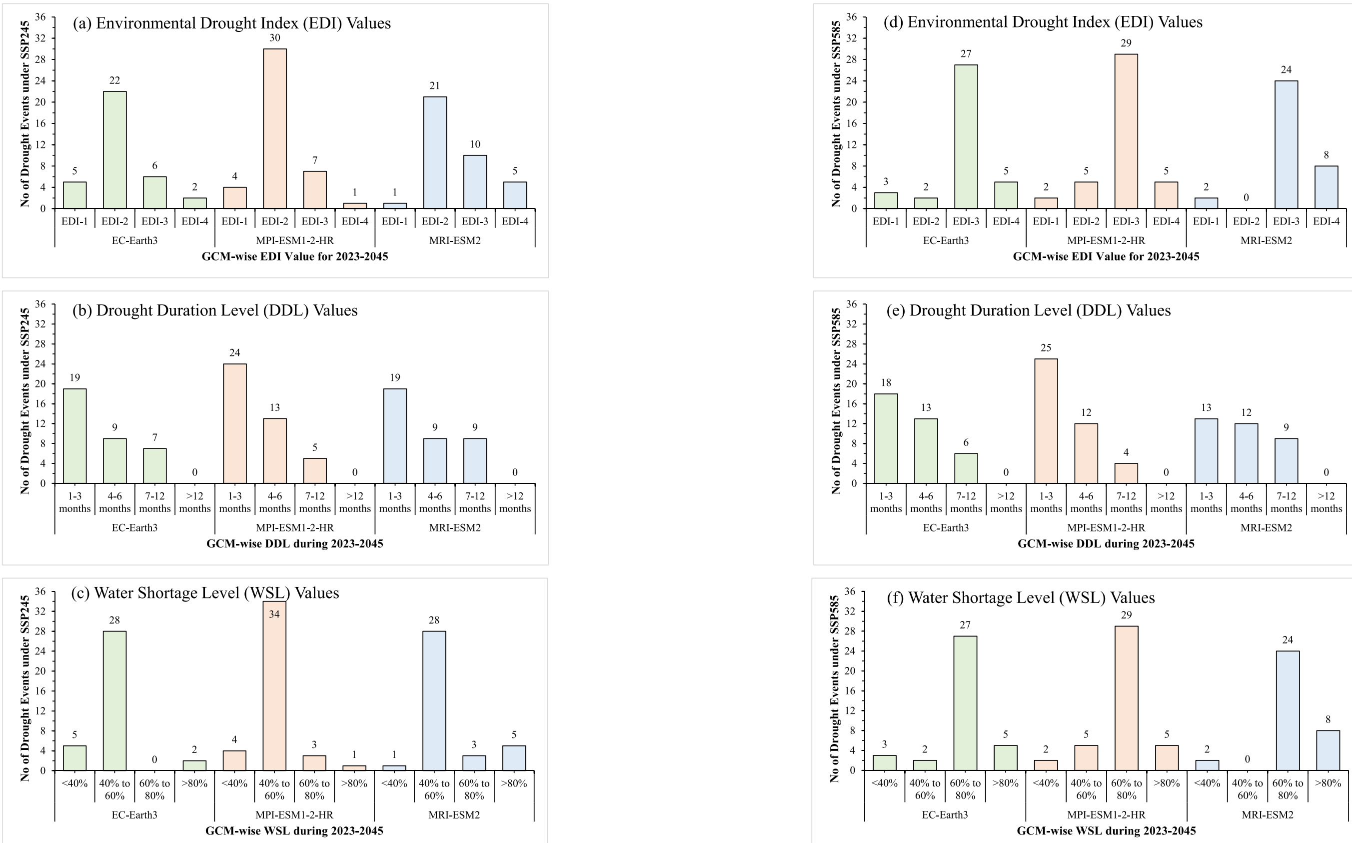

Fig. 11. The numbers of environmental drought events with different EDI values (EDI-1, EDI-2, EDI-3, and EDI-4) and for different lengths of the drought period (DDL in months; 1–3, 4–6, 7–12, and > 12) and for different levels of water shortage (WSL in %; <40, 40–60, 60–80, and > 80) for the three General Circulation Models (GCMs viz., EC-Earth3, MPI-ESM1-2-HR, and MRIESM2) under the two future scenarios [SSP245 (left-side; a to c) and SSP585 (right-side; d to f)] for the second future period (2023–2045) at Jaraikela catchment.

scenario compared to the previous FP-1 scenario. These findings suggest that while moderate drought events continued to dominate during FP-2 under SSP245, there may be an increasing trend in extreme drought occurrences.

During FP-2 under SSP585 [Fig. 12(iii[d, e, f])], all three GCMs identified severe drought (EDI-3) events as the most common, accounting for 73%, 71%, and 71% of total drought events for GCM1, GCM2, and GCM3, respectively. This finding contrasts with the occurrence of moderate drought (EDI-2) events observed under SSP245 and SSP585 of FP-1, as well as SSP245 of FP-2. However, the finding is coherent with the observed period, where both severe and moderate drought percentages were comparable and dominant. This result is critical and contrasts with all the discussions done so far, given that GCM2 under SSP585 was identified as the best representative model of the observed condition over the Jaraikela catchment, which itself indicated severe drought events (EDI-3) as the most common type during 2023–2045. The fundamental cause behind severe droughts was identified as the water shortage level ranging between 40% and 60% (WSL-2), which was a significant driver of drought severity during FP-2. Additionally, the most prominent DDL category identified in FP-2 under SSP585 was the occurrence of quaternary drought (DDL-1) events. Moreover, there was an increased percentage of extreme drought (EDI-4) events identified by GCM1 (14%), GCM2 (12%), and GCM3 (24%) under SSP585 compared to the previous scenarios. Overall, the findings presented in the above discussion align well with the results reported in Section 4.6, providing further confidence in the accuracy and reliability of the findings. These insights emphasize the importance of considering different climate scenarios and GCMs to comprehensively assess the potential changes in drought characteristics over time, enabling better preparedness and adaptation strategies for future environmental drought events.

5.2. Analysis of month-wise variations in environmental drought events

Table 4 provides a comprehensive comparison of the EDI severity levels for each month across the observed period and the two future periods, allowing for insights into the changes in drought conditions [in terms of frequency of EDI (Table 4a) and percentage contribution of each EDI (Table 4b)] over time in the Jaraikela catchment. In this analysis, the observed period was compared with the GCM2 model outputs under the SSP585 scenario, as GCM2 was identified as the closest match to the observed conditions.

During the 35-year observed period, the months falling under the LFS - from November to May –exhibited a high number of severe drought (EDI-3) events, ranging from 13 to 17 occurrences. These severe droughts constituted 37% to 49% of all environmental drought types during this period. Following severe droughts, moderate droughts (EDI-2) ranged from 13 to 16 events (excluding November and December), occupying 37% to 46% of the total environmental drought types. This analysis indicated that these LFS months were susceptible to prolonged and severe environmental drought conditions, posing challenges to water availability. Certain months, such as June during the HFS and November and December in the LFS, displayed intermittent occurrences of severe (EDI-3), moderate (EDI-2), and slight (EDI-1) droughts. These sporadic drought events may affect agricultural activities and water availability during critical periods, such as the beginning of the Kharif or Rabi cropping seasons. On the other hand, months under HFS (June to October) showed a high number of non-drought events, ranging from 20

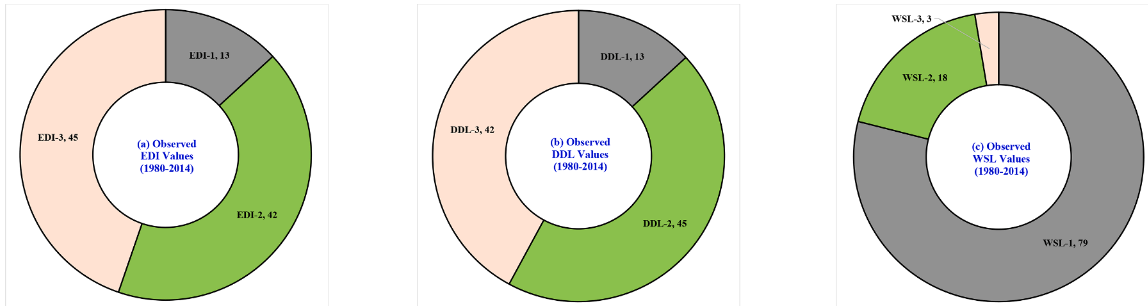

(i) Observed percentage of EDI (a), DDL (b), and WSL (c) values for the observed period 1980-2014

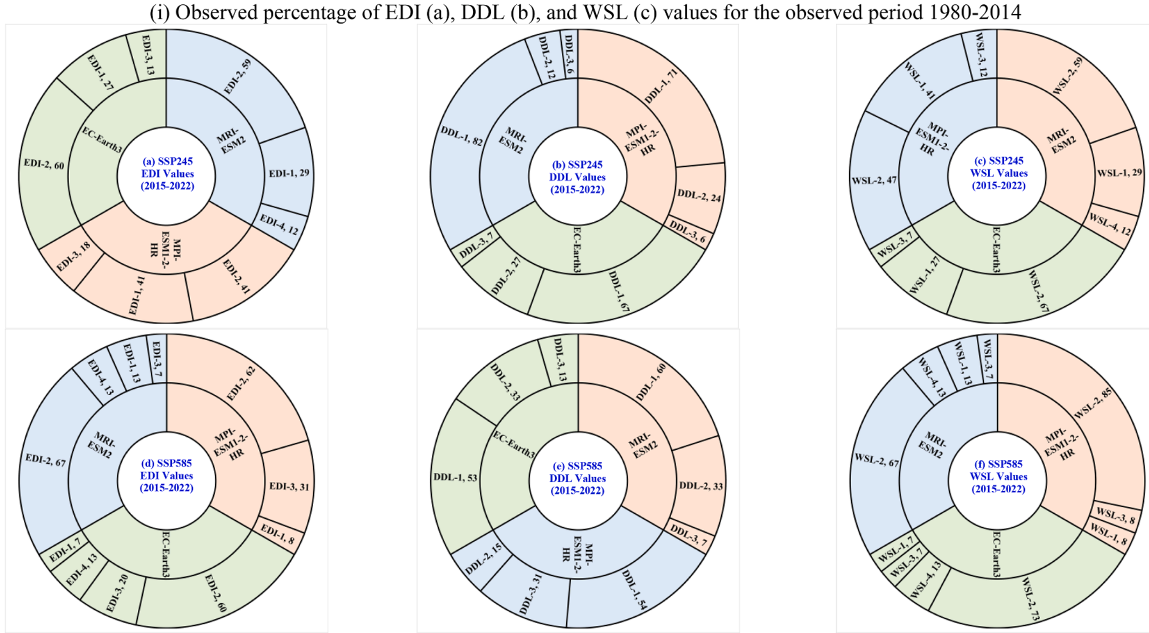

(ii) Future percentage of EDI (a, d), DDL (b, e), and WSL (c, f) values for the period 2015-2022 under SSP245 (a, b, c) and SSP585 (d, e, f)

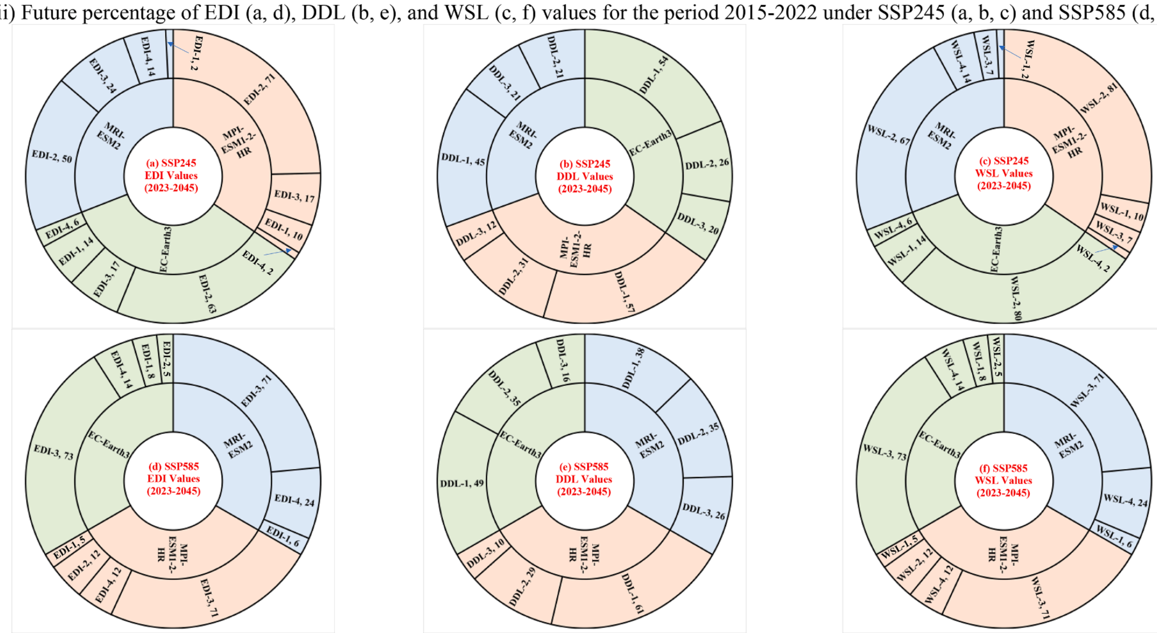

(iii) Future percentage of EDI (a, d), DDL (b, e), and WSL (c, f) values for the period 2023-2045 under SSP245 (a, b, c) and SSP585 (d, e, f)

Fig. 12. Comparative analysis between the observed period (i) and the two future periods (ii and iii) for recording the percentage contribution of each drought characteristic in the Jaraikela catchment [Note: numbers next to the comma inside each sunburst plot indicate the percentage of the drought characteristics (like EDI, DDL, and WSL)].

Table 4
Month-wise frequency (a) and percentage (b) analysis of Environmental Drought Index (EDI) at various severity levels (EDI-1: Slight; EDI-2: Moderate; EDI-3: Severe; EDI-4: Extreme; EDI-0: No Drought) during the observed period (1980–2014), future period (FP) – 1 (2015–2022), and FP-2 (2023–2045) at Jaraikela catchment; for FP-1 and FP-2, GCM2 named MPI-ESM1-2-HR under SSP585 is considered for comparative analysis, given it was identified the best representative model [Note: June to October represents High Flow Season (HFS); the shades from green to yellow to orange to red indicates increasing number of corresponding EDI events].

(a) Frequency analysis of different EDI types

Months	Observed Period (1980-2014)					FP-1 (2015-2022) of GCM2 under SSP585					FP-2 (2023-2045) of GCM2 under SSP585				
	EDI-0	EDI-1	EDI-2	EDI-3	EDI-4	EDI-0	EDI-1	EDI-2	EDI-3	EDI-4	EDI-0	EDI-1	EDI-2	EDI-3	EDI-4
January	5	1	13	16	0	0	0	4	4	0	4	0	1	15	3
February	1	1	16	17	0	3	0	1	4	0	4	0	1	14	4
March	2	0	16	17	0	1	1	2	4	0	9	0	1	11	2
April	0	2	16	17	0	1	0	3	4	0	4	1	3	13	2
May	1	2	15	17	0	3	0	3	2	0	9	2	4	6	2
June	20	2	3	10	0	7	0	1	0	0	22	0	0	0	1
July	34	0	0	1	0	8	0	0	0	0	23	0	0	0	0
August	35	0	0	0	0	8	0	0	0	0	23	0	0	0	0
September	35	0	0	0	0	8	0	0	0	0	23	0	0	0	0
October	33	0	0	2	0	3	0	2	3	0	12	0	0	7	4
November	21	0	1	13	0	0	0	4	4	0	2	0	1	17	3
December	10	2	7	16	0	0	0	4	4	0	0	0	1	19	3

(b) Percentage contribution of different EDI types

Months	Observed Period (1980-2014)					FP-1 (2015-2022) of GCM2 under SSP585					FP-2 (2023-2045) of GCM2 under SSP585				
	EDI-0	EDI-1	EDI-2	EDI-3	EDI-4	EDI-0	EDI-1	EDI-2	EDI-3	EDI-4	EDI-0	EDI-1	EDI-2	EDI-3	EDI-4
January	14%	3%	37%	46%	0%	0%	0%	50%	50%	0%	17%	0%	4%	65%	13%
February	3%	3%	46%	49%	0%	38%	0%	13%	50%	0%	17%	0%	4%	61%	17%
March	6%	0%	46%	49%	0%	13%	13%	25%	50%	0%	39%	0%	4%	48%	9%
April	0%	6%	46%	49%	0%	13%	0%	38%	50%	0%	17%	4%	13%	57%	9%
May	3%	6%	43%	49%	0%	38%	0%	38%	25%	0%	39%	9%	17%	26%	9%
June	57%	6%	9%	29%	0%	88%	0%	13%	0%	0%	96%	0%	0%	0%	4%
July	97%	0%	0%	3%	0%	100%	0%	0%	0%	0%	100%	0%	0%	0%	0%
August	100%	0%	0%	0%	0%	100%	0%	0%	0%	0%	100%	0%	0%	0%	0%
September	100%	0%	0%	0%	0%	100%	0%	0%	0%	0%	100%	0%	0%	0%	0%
October	94%	0%	0%	6%	0%	38%	0%	25%	38%	0%	52%	0%	0%	30%	17%
November	60%	0%	3%	37%	0%	0%	0%	50%	50%	0%	9%	0%	4%	74%	13%
December	29%	6%	20%	46%	0%	0%	0%	50%	50%	0%	0%	0%	4%	83%	13%

to 35, encompassing 57% to 100% of all environmental drought types. The monsoonal season generally provided sufficient water resources, ensuring that droughts are less likely to occur during this period. However, an exception was observed in June, which exhibited 29% of severe drought EDI-3) events compared to zero for other months under HFS. Nonetheless, no instances of extreme droughts (EDI-4) were recorded during the observed period. These findings serve as a baseline for comparing future drought occurrences and patterns.

During the eight years (FP-1) under the SSP585 scenario, the frequency and intensity of drought events mainly followed the pattern shown during the observed period. The catchment experienced severe drought (EDI-3) conditions in the early months of the year, specifically from January to April, with around 50% of all the environmental drought types. This indicates a slight shift towards more severe drought conditions during the first few months of the year compared to the observed period. Moreover, in contrast to the observed period, FP-1 showed an increase in the occurrence of both severe (EDI-3) and moderate drought (EDI-2) events during the winter months (October to December), ranging around 50% of all the environmental drought types. This suggested that the projected scenario made the winter season more susceptible to severe droughts. Nonetheless, and similar to the observed period, no instances of extreme droughts (EDI-4) were recorded during the FP-1. In fact, the same was exhibited for slight drought (EDI-1) events. These findings serve as a baseline for comparing future drought occurrences and patterns. The results obtained from FP-1 underscore the significance of ongoing monitoring and research to holistically comprehend the dynamic patterns of drought events within the catchment. To gain a more comprehensive understanding of future drought occurrences, it becomes imperative to analyze FP-2.

Over the 23 years of FP-2 under the SSP585 scenario, notable changes in drought patterns were observed in the Jaraikela catchment. Months from January to April consistently exhibited a high proportion of severe drought (EDI-3) events, comprising around 60% of all environmental drought types, increasing to around 80% during November and December. This indicated a potential shift towards more severe drought conditions during these months compared to the observed period and FP-1. This alteration from moderate drought (EDI-2) during FP-1 to severe drought (EDI-3) events during FP-2 suggested a concerning inclination of increasing severity during the initial and later months of the year. Remarkably, all months, except for the monsoonal months, showed occurrences of extreme drought (EDI-4) events ranging from 9% to 17%. This contrasted with the patterns observed during the observed period and both scenarios of FP-1. Additionally, the proportion of non-drought (EDI-0) events declined significantly during FP-2, especially during the LFS, indicating a deteriorating trend with increased occurrences of severe droughts and reduced non-drought events. On a positive note, July, August, and September remained free from any drought occurrences (i.e., EDI-0) during FP-2, aligning consistently with the observed period and FP-1. Overall, the findings from FP-2 underscore the likelihood of changes in drought patterns and an escalation in severity within the Jaraikela catchment under the SSP585 scenario. These insights emphasize the urgency of implementing proactive and adaptive water resource management strategies to tackle the region's potential environmental drought challenges. Continuous monitoring and research will be indispensable to better comprehend and respond to the evolving dynamics of drought in the catchment.

5.3. Analyzing the sensitivity of EDI toward SFR

The EDI is found to be sensitive to the SFR (both the observed and simulated SFR) through its calculation process, which involves comparing the observed and simulated SFR with the MFR. Enlisted below are the step-wise sensitivity reflections of EDI toward SFR:

- The first step involves calculating the DDL. The SFR is compared to the MFR for each month during this step. If the observed SFR falls below the MFR, it signifies a water deficit or the presence of drought for that month. The consecutive months with such deficits are counted to determine the duration of the drought event. This calculation directly reflects the sensitivity of EDI to variations in observed SFR. If the observed SFR fluctuates, it will impact the duration and intensity of the drought events identified by the EDI.
- The next step involves calculating the WSL. This component of the EDI quantifies the severity of the drought events in terms of percentage water availability. It considers the largest water deficit observed during the DDL and relates it to the maximum MFR within the same DDL. The largest water deficit is the largest negative difference between SFR and MFR. Thus, the sensitivity of the EDI to variations in SFR is directly reflected in the WSL component, in that the greater the absolute value between the SFR and MFR, the greater the WSL value.
- The final step is the integration of DDL and WSL to calculate the overall EDI value for each environmental drought event. The EDI categorizes these events into four levels of severity (slight, moderate, severe, and extreme) based on the DDL and WSL values. Given the direct relation of DDL and WSL with SFR, it can be mathematically proclaimed that the sensitivity of EDI to SFR plays a pivotal role in determining the severity levels and classifications of environmental drought events.

In summary, variations in SFR, whether observed or simulated, directly influence the identification, duration, and severity assessment of environmental drought events by the EDI. This sensitivity underscores the importance of accurate and reliable SFR data, both observed and simulated, in assessing environmental drought using the EDI.

5.4. Evidence from elsewhere studies: Need for adaptation measures

Several recently published works have widely reported and affirmed the results discussed in the previous sections, more specifically in the context of the Brahmani River basin, whose part is the Jaraikela catchment. Utilizing an Integrated Drought Index (IDI), Shah and Mishra (2020) identified the three most severe drought events in the Brahmani River basin, occurring in 1966, 1979, and 2010. Notably, the 2010 drought emerged as the most recent severe event, encompassing the period from November 2008 to June 2011. Moreover, their projections suggested an anticipated rise in drought frequency based on the IDI under the influence of a warming climate. These results reinforce the observations presented in Figs S3 and 6, lending additional support to the documented environmental drought pattern. Ganguli et al. (2022) found that catchments in eastern peninsular India, including Brahmani, Baitarani, etc. River basins experienced prolonged hydrological droughts lasting over two months, with varying frequencies of 15 to 30 occurrences during 1965–2019. This aligns with the presented frequency analysis of EDI, shown in Table 4 and Figs S3, 6, S6, and 12. Vandana et al. (2019) projected rising annual mean temperatures of 0.8–1.0, 1.5–2.0, and 2.0–3.3°C in the 2020s, 2050s, and 2080s, respectively, and annual rainfall to fluctuate between −1.6% and 8.1% in the same periods. These findings highlighted potential changes in the climate conditions for the Jaraikela catchment in the coming decades. Numerous other studies (Amrit et al., 2018; Islam et al., 2012; Sinha et al., 2020; Swain et al., 2020) have provided substantial evidence of the persistent occurrences of hydrological, meteorological, and agricultural droughts in the study basin and catchment, reinforcing the significance of the presented findings on environmental droughts. The implementation of the EDI represented the novel part of the present investigation. For robustness and comparability, future researchers may adopt this methodology to validate the findings by considering other catchment and river basins.

Moreover, the Brahmani River basin, in general, and the Jaraikela catchment, in particular, lack dedicated research into the ecological and environmental dimensions of drought impacts. Although this study offers insights into environmental drought events from 1980 to 2014 and the observed period of 2015 to 2018, besides future drought occurrences, it's crucial to recognize that in-depth assessments of ecological health and direct water unavailability impact due to environmental droughts require specialized interdisciplinary research. In alignment with this perspective, the present study undertook a review of recent media reports to enhance the validation of environmental drought impacts on the ecological health of the study basin. Since 2015, the Brahmani River basin has faced mounting ecological and environmental challenges, as per the media reports.[2] Post-monsoon periods have witnessed paddy crop burning due to elevated temperatures, reaching nearly 50°C, exacerbated by fluoride-bearing gases. The land has been converted into ash ponds, and solid waste disposal facilities have mushroomed, rendering once fertile agricultural land barren. Groundwater depletion from mining activities has triggered severe water shortages in surrounding villages. Rapid industrialization and mining have plunged around 600,000 people in the Brahmani and Mahanadi basins into a severe water crisis. Deprived of Brahmani River water for drinking and irrigation, these communities bear the brunt of water

[2] The information regarding the impact of water scarcity and drought events in the Brahmani River basin, mainly the Jaraikela catchment, and across the vicinity of Jharkhand and Odisha states of India has been gathered from some of the leading newspapers of India and popular web pages of Government and Non-Governmental Organizations (NGOs). This included – 'The Bastion' (https://thebastion.co.in/politics-and/how-development-in-jharkhand-contributed-to-a-water-crisis/, accessed in November 2023), 'Disaster Management Department' (https://disaster.jharkhand.gov.in/drought.php, accessed in November 2023), 'The Pioneer' (https://www.dailypioneer.com/2015/state-editions/pipe-water-supply-from-mahanadi-brahmani-rivers-demanded.html, accessed in November 2023), 'The Economics Times' (https://economictimes.indiatimes.com/news/politics-and-nation/orissa-to-become-water-stressed-state-by-2015/articleshow/6320448.cms?from=mdr, accessed in November 2023), 'India Water Portal' (https://www.indiawaterportal.org/articles/industrial-effluents-dirty-river-brahmani, accessed in November 2023), and 'Mongabay' (https://india.mongabay.com/2022/03/odishas-kharasrota-river-stuck-in-tussle-between-protecting-ecology-and-providing-drinking-water/, accessed in November 2023).

allocation to industries and coal mines. Approval of 13 industrial projects, some tapping Brahmani, Mahanadi, and Sabari Rivers, heightens concerns about sustainable water use. Compounding these issues is the lack of industry water use data, necessitating transparent water allocation and a White Paper on Water Availability. Over six decades, water availability has declined by 75%, endangering food security, driving migration, and harming vulnerable populations. Stringent enforcement of environmental laws is critical to combat deforestation and environmental damage. To address these challenges, experts propose thousands of micro-dams in upper Brahmani and Baitarani river catchments to bolster aquifer storage and year-round freshwater flow. Instream and catchment-based measures can recharge the basin sustainably. Integrated, multidisciplinary assessments should precede large-scale water extraction projects to ensure viability while safeguarding ecology and communities. Changing public attitudes toward river conservation is vital to avert a looming drinking water shortage.

To this end, this study thus proposes some dedicated recommendations on adaptation to rising environmental drought events in the Jaraikela catchment (discussed in Table 5). Integrating 'Water Resource Management' practices in the Jaraikela catchment is essential to optimize water usage and allocation. Implementing 'Drought Early Warning Systems' will enhance preparedness and response to potential drought events. Embracing 'Climate-Resilient Agriculture' with drought-tolerant crops and efficient irrigation can bolster food security. 'Ecosystem Restoration' efforts, such as afforestation, will be crucial in maintaining water availability. Promoting 'Water Use Efficiency measures,' like water-saving technologies, is necessary to reduce water demand. 'Capacity Building and Awareness' programs are vital for educating communities and policymakers about drought risks and adaptive strategies. Encouraging 'Diversification of Livelihoods' will reduce dependency on agriculture during droughts. 'Inter-basin Cooperation' can lead to effective water management among neighboring catchments. Although challenges exist while augmenting these adaptive measures on the field, as discussed in the last column of Table 5, combining these nature-based solutions with region-specific traditional practices can create a holistic approach to enhance resilience to drought events in the Jaraikela catchment. These recommendations align with IPCC assessment reports (IPCC, 2022) and can contribute to sustainable water resource management and adaptation strategies in the face of ongoing and future environmental drought challenges.

5.5. Complexity of environmental drought: A way forward

The scientific literature has shown limited efforts in explicitly addressing the measurement and characterization of environmental drought through the development of comprehensive indices, as also emphasized by Crausbay et al. (2017), Shi et al. (2018), and Vicente-Serrano et al. (2020). There could be several reasons why environmental drought has not received the same level of attention as meteorological, hydrological, and agricultural droughts have received for many decades, and socioeconomic droughts have received recently. A few of the reasons could be: One, developing a comprehensive and universally accepted definition and framework for environmental drought may have posed challenges due to the diversity and complexity of ecosystems worldwide. The lack of consensus on the precise parameters and indicators required to quantify and monitor environmental drought could have hindered the development of dedicated indices. Two, environmental drought is inherently complex and influenced by a multitude of factors, including climate, hydrology, land cover, and human activities. Understanding the intricate interactions and feedback mechanisms between these components requires comprehensive research and integration of diverse disciplines, which may have posed challenges in developing dedicated indices. Three, the traditional classification of drought types has predominantly focused on human-centric perspectives, overlooking the ecological dimensions of drought. This human-centric approach may have overshadowed the need to specifically

Table 5
Adaptation measures for mitigating ongoing and future environmental drought events in the Jaraikela catchment.

Adaptive measures	Description	Possible challenges to overcome
Integrated Water Resource Management	Implementing an Integrated Water Resource Management approach considering surface water and groundwater resources. This includes sustainable water extraction practices, rainwater harvesting, and improved water storage infrastructure to ensure better water availability during drought periods.	Limited financial resources, technological and infrastructural limitations, institutional and policy barriers, social and cultural acceptance, climate variability, environmental impact and trade-offs, legal and regulatory constraints, intersectoral conflicts, and ensuring long-term sustainability.
Drought Early Warning Systems	Establishing and strengthening drought early warning systems enhances preparedness and response to potential drought events. These systems should utilize remote sensing technologies, weather forecasting, and monitoring key indicators such as EDI, DDL, and WSL to provide timely information to decision-makers and stakeholders.	Data availability and reliability, technical expertise and capacity, funding and maintenance, coordination between agencies, translating early warnings into actionable responses, engaging communities, addressing false alarms and complacency, and ensuring information dissemination to vulnerable populations.
Climate-Resilient Agriculture	Promoting climate-resilient agricultural practices, such as drought-tolerant crop varieties, efficient irrigation methods, agroforestry, and soil moisture conservation techniques. This will help minimize the impact of droughts on agriculture and ensure food security.	Farmer awareness and adoption of new practices, access to and affordability of drought-tolerant crop varieties, water availability for irrigation, technical support, financial resources, market linkages for resilient crops, climate variability, and ensuring inclusivity of smallholder farmers in adaptation efforts.
Ecosystem Restoration	Implementing ecosystem restoration initiatives, such as afforestation, reforestation, and sustainable land management practices. Healthy ecosystems are crucial in maintaining water availability and regulating water flow during dry periods.	Securing sufficient land for restoration, addressing competing land-use demands, ensuring community engagement and participation, overcoming resource constraints, monitoring and ensuring the effectiveness of restoration efforts, and addressing potential risks of introducing non-native species during afforestation and reforestation.
Water Use Efficiency	Encouraging water use efficiency in all sectors, including agriculture, industry, and domestic use. Implementing water-saving technologies and water recycling, practices can reduce water demand and increase resilience to drought events.	Initial costs of adopting water-saving technologies, ensuring behavioral change and adoption of water-efficient practices, addressing infrastructure limitations for water recycling, considering equity and social aspects of water use, and integrating water use efficiency measures across different sectors while ensuring sustainable economic growth and development.
Capacity Building and Awareness	Conducting capacity-building programs and awareness campaigns to educate communities, farmers, and policymakers	Resource constraints for conducting extensive capacity-building programs and awareness campaigns, ensuring effective

(continued on next page)

Table 5 (*continued*)

Adaptive measures	Description	Possible challenges to overcome
	about drought risks and adaptive strategies. This will foster a culture of resilience and preparedness within the catchment.	communication and engagement with diverse stakeholders, addressing knowledge gaps and overcoming resistance to change, and sustaining a long-term commitment to ensure continuous learning and adaptation within the catchment community.
Diversification of Livelihoods	In rural communities, advocating for livelihood diversification can reduce dependency on agriculture during droughts. Local economies become more resilient by promoting less water-intensive alternative income-generating activities, such as cottage industries, eco-tourism, and renewable energy projects. This approach enhances economic stability, fosters sustainable practices, and mitigates drought impacts on food security.	Resistance to change from traditional agricultural practices, lack of awareness about alternative income-generating activities, limited access to resources and capital for starting new ventures, and the need for skill development and training in diverse fields. Overcoming these challenges requires effective community engagement, capacity-building programs, and supportive policies and funding mechanisms.
Inter-basin Cooperation	Encouraging collaboration and information sharing among neighboring catchments and basins to address drought challenges collectively. Such cooperation can lead to more effective water management and equitable distribution during droughts.	Negotiating complex water-sharing agreements among different catchments, overcoming political and institutional barriers to cooperation, ensuring equitable distribution of water resources, addressing competing interests and conflicting priorities among stakeholders, and establishing effective communication and coordination mechanisms between neighboring basins.

address the impacts of drought on ecosystems and the services they provide. Addressing these challenges requires interdisciplinary research and a comprehensive understanding of the interactions between climate, hydrology, and the environment. Moreover, the increasing influence of climate change on global ecosystems highlights the urgency of adopting proactive measures to understand and mitigate environmental drought's impacts holistically.

The terminology "environmental drought" employed in this study is a deliberate choice intended to align with the specific research focus. It signifies a hydrological condition in river ecosystems where crucial components, such as flow requirements and aquatic elements, become stressed due to a deficit in available water resources. This terminology underscores the unique and valuable contribution of the present research, which is exclusively dedicated to evaluating river ecosystem health and a comprehensive understanding of the environmental consequences of reduced streamflow. This is particularly vital in the context of potential climate change scenarios, where these ecosystems are vulnerable to shifts in water availability. In contrast, traditional assessments of ecological drought tend to adopt a broader perspective, encompassing terrestrial ecosystems in addition to river ecosystems. However, this study's approach is highly specialized, focusing explicitly on assessing the health and adaptability of river ecosystems in response to alterations in streamflow conditions. In this regard, the terminology "environmental drought" aptly characterizes this research's specific scope and objectives, signifying how changes in streamflow impact river ecosystems and their ecological well-being.

Nonetheless, like any research endeavor, the present study has certain limitations that have been acknowledged as potential areas for future research. Limitations of this study include uncertainties arising from the selection of GCMs for future projections, leading to varied outcomes for environmental drought predictions. Ensuring robust GCM selection is crucial for accuracy. Additionally, developing the EDI involved parameterizing variables and thresholds, influencing sensitivity and performance. Proper validation and sensitivity analyses were essential, which can be accounted for in future work. Evaluating the EDI's effectiveness at the catchment scale against existing indices and observed data is critical. Though historical validation opportunities were limited due to its novelty, credibility can be enhanced through comparisons with other drought indices. To emphasize further and more specifically, one of the challenges faced by this study is the lack of a recognized environmental drought index in the scientific literature for comparison with the EDI. This constrained the present study to perform direct quantitative comparisons. Besides, interpreting specific drivers of environmental drought using the EDI alone is challenging and may necessitate additional research, such as hydrological modeling and land-use change assessments, for a comprehensive understanding of underlying mechanisms. Additionally, as the primary objective of this study was to assess the applicability of the novel EDI, with a specific focus on the Jaraikela station, expanding the analysis to encompass the entire Brahmani River basin using the EDI offers a promising avenue for enhancing the scientific understanding on the spatial extent of environmental drought and its implications. This extended investigation will significantly contribute to providing a more nuanced perspective on environmental drought dynamics and their far-reaching consequences.

6. Conclusions

The present study pioneered the development of the Environmental Drought Index (EDI) and thoroughly investigated the variations in distribution and characteristics of environmental drought events in the Jaraikela catchment of the Brahmani River Basin, India. Moreover, the study examined EDI under different emission scenarios (SSP245 and SSP585) and multiple General Circulation Models (GCMs) across observed periods (1980–2014) and two future periods (FP-1: 2015–2022 and FP-2: 2023–2045). The EDI was primarily based on water shortage (WSL) and drought duration (DDL) levels as crucial indicators. To obtain the EDI, the investigation utilized observed Streamflow Rate (SFR) data and employed the HCCS model for generating simulated streamflow for all study periods. The objective was to specifically consider the environmental aspect of droughts, for which Tennant's method was adopted to estimate the environmental flow requirements necessary to sustain the Koel River flow in the catchment. Comparing the Minimum in-stream Flow Requirements (MFR) with the SFR, the study could determine the different categories of environmental droughts. The study successfully validated the simulated EDI values against the observed EDI values and identified GCM2, referred to as "MPI-ESM1-2-HR" under SSP585, as the most accurate representation of the present observed environmental drought conditions in the study area. To this end, the study draws the following conclusions:

- The HCCS model demonstrated its effectiveness in simulating streamflow rates, which was a crucial input for developing the EDI. Through the implementation of the HCCS model, the study successfully estimated the MFR required to sustain the Koel River flow in the Jaraikela catchment.
- Findings from flow hydrographs indicated that the Jaraikela catchment mostly experienced no environmental drought (EDI-0) during monsoonal months, with SFR significantly higher than the MFR. However, during non-monsoonal periods, SFR was lower than MFR, indicating potential environmental drought.
- Historical drought analysis indicated that between 1980 and 2014, the Jaraikela catchment experienced 38 environmental drought

events annually, predominantly during non-monsoonal seasons. Severe (EDI-3) and moderate (EDI-2) droughts were the most frequent, impacting water availability and ecological health. DDL had a greater impact on the EDI than WSL, affecting the degree of drought severity. No extreme environmental drought events (EDI-4) were observed, indicating the absence of exceptionally severe and prolonged droughts during the study period.
- The analysis of the percentage contribution of different EDI types to overall environmental drought revealed that during FP-2 under SSP585, severe drought (EDI-3) events were the most common, accounting for 71–73 % of total drought occurrences across all three GCMs. This finding contrasted with the prevalence of moderate droughts (EDI-2) observed in SSP245 of FP-2 and both scenarios of FP-1 but aligned with the distribution during the observed period.
- GCM2 under SSP585 also exhibited severe drought (EDI-3) dominance during FP-2, reflecting its representation of observed period conditions. Severe drought prevalence in FP-2 was primarily driven by water shortage levels ranging from 40% to 60% (WSL-2). There was a noteworthy increase in the percentage of extreme drought (EDI-4) events under SSP585 in GCM1 (14%), GCM2 (12%), and GCM3 (24%), a trend not observed during the observed period and in both scenarios of FP-1.
- The month-wise analysis of FP-2 under the SSP585 scenario indicated that the months from January to April and October to December consistently exhibited a high proportion of severe drought (EDI-3) events, signaling a potential shift towards increasing severity compared to the observed period, and both scenarios of FP-1. Additionally, extreme drought (EDI-4) events were observed in all months except the monsoonal months, indicating a contrasting trend with the observed period and FP-1. However, the positive observation was that July, August, and September remained free from any drought occurrences (EDI-0) during FP-2, which was consistent with the observed period and FP-1.
- The study thus proposed several adaptive measures to mitigate the impacts of increasing environmental drought events in the Jaraikela catchment, including integrated water resource management, drought early warning systems, climate-resilient agriculture, ecosystem restoration, water use efficiency, capacity building and awareness, diversification of livelihoods, and inter-basin cooperation. These measures are aimed at enhancing water availability, promoting sustainable practices, and fostering resilience in the face of future drought challenges.

Declaration of Generative AI and AI-assisted technologies in the writing process. During the preparation of this work, the authors used the 'OpenAI' platform in order to improve language. After using this service, the authors reviewed and edited the content as needed and took full responsibility for the content of the publication

Funding

This work is partially supported by the Ministry of Earth Sciences (MoES), under the Government of India (MoES/PAMC/H&C/124/2019-PC-II). The funding for the student (Aman Srivastava) was supported by the Prime Minister's Research Fellowship (PMRF/2401746/21CE91R03) under the Ministry of Education, Government of India.

Declaration of competing interest

The authors declare that they have no known competing financial interests or personal relationships that could have appeared to influence the work reported in this paper.

Data availability

Data is already available in some open repository as mentioned in the manuscript

Appendix A. Supplementary data

Supplementary data to this article can be found online at https://doi.org/10.1016/j.jhydrol.2023.130462.

References

Amrit, K., Mishra, S.K., Pandey, R.P., 2018. Tennant concept coupled with standardized precipitation index for environmental flow prediction from rainfall. J. Hydrol. Eng. 23 (2), 05017031. https://doi.org/10.1061/(ASCE)HE.1943-5584.0001605.

Anil, S., Manikanta, V., Pallakury, A.R., 2021. Unravelling the influence of subjectivity on ranking of CMIP6 based climate models: A case study. Int. J. Climatol. 41 (13), 5998–6016. https://doi.org/10.1002/joc.7164.

Bae, H., Ji, H., Lim, Y.J., Ryu, Y., Kim, M.H., Kim, B.J., 2019. Characteristics of drought propagation in South Korea: Relationship between meteorological, agricultural, and hydrological droughts. Nat. Hazards 99 (1), 1–16. https://doi.org/10.1007/s11069-019-03676-3.

Bhagwat, P.P., Maity, R., 2014. Development of HydroClimatic Conceptual Streamflow (HCCS) model for tropical river basin. J. Water Clim. Change 5 (1), 36–60. https://doi.org/10.2166/wcc.2013.015.

Chiang, F., Mazdiyasni, O., AghaKouchak, A., 2021. Evidence of anthropogenic impacts on global drought frequency, duration, and intensity. Nat. Commun. 12 (1), 2754. https://doi.org/10.1038/s41467-021-22314-w.

Crausbay, S.D., Ramirez, A.R., Carter, S.L., Cross, M.S., Hall, K.R., Bathke, D.J., et al., 2017. Defining ecological drought for the twenty-first century. Bull. Am. Meteorol. Soc. 98 (12), 2543–2550. https://doi.org/10.1175/BAMS-D-16-0292.1.

Di Virgilio, G., Ji, F., Tam, E., Nishant, N., Evans, J.P., Thomas, C., et al., 2022. Selecting CMIP6 GCMs for CORDEX dynamical downscaling: Model performance, independence, and climate change signals. Earth's. Future 10 (4), e2021EF002625. https://doi.org/10.1029/2021EF002625.

Ganguli, P., Singh, B., Reddy, N.N., Raut, A., Mishra, D., Das, B.S., 2022. Climate-catchment-soil control on hydrological droughts in peninsular India. Sci. Rep. 12 (1), 8014. https://doi.org/10.1038/s41598-022-11293-7.

Guo, Y., Huang, S., Huang, Q., Wang, H., Fang, W., Yang, Y., Wang, L., 2019. Assessing socioeconomic drought based on an improved Multivariate Standardized Reliability and Resilience Index. J. Hydrol. 568, 904–918. https://doi.org/10.1016/j.jhydrol.2018.11.055.

Hagenlocher, M., Meza, I., Anderson, C.C., Min, A., Renaud, F.G., Walz, Y., et al., 2019. Drought vulnerability and risk assessments: state of the art, persistent gaps, and research agenda. Environ. Res. Lett. 14 (8), 083002. https://iopscience.iop.org/article/10.1088/1748-9326/ab225d/meta.

Haile, G.G., Tang, Q., Li, W., Liu, X., Zhang, X., 2020. Drought: Progress in broadening its understanding. Wiley Interdiscip. Rev. Water 7 (2), e1407.

IPCC (2022). Climate Change 2022: Impacts, Adaptation, and Vulnerability. Contribution of Working Group II to the Sixth Assessment Report of the Intergovernmental Panel on Climate Change [H.-O. Pörtner, D.C. Roberts, M. Tignor, E.S. Poloczanska, K. Mintenbeck, A. Alegría, M. Craig, S. Langsdorf, S. Löschke, V. Möller, A. Okem, B. Ra-ma (eds.)]. Cambridge University Press. Cambridge University Press, Cambridge, UK and New York, NY, USA, 3056 pp., doi:10.1017/9781009325844.

Iqbal, Z., Shahid, S., Ahmed, K., Ismail, T., Ziarh, G.F., Chung, E.S., Wang, X., 2021. Evaluation of CMIP6 GCM rainfall in mainland Southeast Asia. Atmos. Res. 254, 105525 https://doi.org/10.1016/j.atmosres.2021.105525.

Islam, A., Sikka, A.K., Saha, B., Singh, A., 2012. Streamflow response to climate change in the Brahmani River Basin. India. Water Resources Management 26 (6), 1409–1424. https://doi.org/10.1007/s11269-011-9965-0.

Jiang, T., Su, X., Singh, V.P., Zhang, G., 2022. Spatio-temporal pattern of ecological droughts and their impacts on health of vegetation in Northwestern China. J. Environ. Manage. 305, 114356 https://doi.org/10.1016/j.jenvman.2021.114356.

Karl, T.R., 1986. The sensitivity of the Palmer Drought Severity Index and Palmer's Z-index to their calibration coefficients including potential evapotranspiration. J. Clim. Appl. Meteorol. 77–86. https://www.jstor.org/stable/26182460.

Kogan, F.N., 1995. Droughts of the late 1980s in the United States as derived from NOAA polar-orbiting satellite data. Bull. Am. Meteorol. Soc. 76 (5), 655–668. https://doi.org/10.1175/1520-0477(1995)076%3C0655:DOTLIT%3E2.0.CO;2.

Liu, S., Shi, H., Sivakumar, B., 2020. Socioeconomic drought under growing population and changing climate: A new index considering the resilience of a regional water resources system. J. Geophys. Res. Atmos. 125 (15), e2020JD033005 https://doi.org/10.1029/2020JD033005.

Ma, F., Yuan, X., Wu, P., Zeng, Z., 2022. A moderate mitigation can significantly delay the emergence of compound hot extremes. J. Geophys. Res. Atmos. 127 (2), e2021JD035427 https://doi.org/10.1029/2021JD035427.

McKee, T. B., Doesken, N. J., & Kleist, J. (1993). The relationship of drought frequency and duration to time scales. In Proceedings of the 8th Conference on Applied Climatology (Vol. 17, No. 22, pp. 179-183). https://climate.colostate.edu/pdfs/relationshipofdroughtfrequency.pdf.

Mehran, A., Mazdiyasni, O., AghaKouchak, A., 2015. A hybrid framework for assessing socioeconomic drought: Linking climate variability, local resilience, and demand. J. Geophys. Res. Atmos. 120 (15), 7520–7533. https://doi.org/10.1002/2015JD023147.

Palmer, W.C., 1965. Meteorological Drought, Vol. 30. US Department of Commerce, Weather Bureau.

Palmer, W.C., 1968. Keeping track of crop moisture conditions, nationwide: the new crop moisture index. Weatherwise 21 (4), 156–161. https://doi.org/10.1080/00431672.1968.9932814.

Reid, K.J., O'Brien, T.A., King, A.D., Lane, T.P., 2021. Extreme water vapor transport during the March 2021 Sydney floods in the context of climate projections. Geophys. Res. Lett. 48 (22), e2021GL095335 https://doi.org/10.1029/2021GL095335.

Saha, A., Pal, S.C., Chowdhuri, I., Roy, P., Chakrabortty, R., Shit, M., 2022. Vulnerability assessment of drought in India: Insights from meteorological, hydrological, agricultural and socio-economic perspectives. Gondw. Res. https://doi.org/10.1016/j.gr.2022.11.006.

Satoh, Y., Yoshimura, K., Pokhrel, Y., Kim, H., Shiogama, H., Yokohata, T., et al., 2022. The timing of unprecedented hydrological drought under climate change. Nat. Commun. 13 (1), 3287. https://doi.org/10.1038/s41467-022-30729-2.

Shafer, B. A., & Dezman, L. E. (1982). Development of surface water supply index (SWSI) to assess the severity of drought condition in snowpack runoff areas. In Proceedings of the 50th Annual Western Snow Conference, Colorado State University, Fort Collins, 1982.

Shah, D., Mishra, V., 2020. Integrated Drought Index (IDI) for drought monitoring and assessment in India. Water Resour. Res. 56 (2), e2019WR026284 https://doi.org/10.1029/2019WR026284.

Shetty, S., Umesh, P., Shetty, A., 2023. The effectiveness of machine learning-based multi-model ensemble predictions of CMIP6 in Western Ghats of India. Int. J. Climatol. https://doi.org/10.1002/joc.8131.

Shi, H., Chen, J., Wang, K., Niu, J., 2018. A new method and a new index for identifying socioeconomic drought events under climate change: A case study of the East River basin in China. Sci. Total Environ. 616, 363–375. https://doi.org/10.1016/j.scitotenv.2017.10.321.

Shukla, S., Wood, A.W., 2008. Use of a standardized runoff index for characterizing hydrologic drought. Geophys. Res. Lett. 35 (2) https://doi.org/10.1029/2007GL032487.

Singh, C., 2023. Intra-seasonal oscillations of South Asian summer monsoon in coupled climate model cohort CMIP6. Clim. Dyn. 60 (1–2), 179–199. https://doi.org/10.1007/s00382-022-06323-z.

Sinha, J., Das, J., Jha, S., Goyal, M.K., 2020. Analysing model disparity in diagnosing the climatic and human stresses on runoff variability over India. J. Hydrol. 581, 124407 https://doi.org/10.1016/j.jhydrol.2019.124407.

Sivakumar, M. V. K., Raymond P., Motha, R., Wilhite, D., & Wood, D. (2011). Agricultural Drought Indices. Proceedings of the WMO/UNISDR Expert Group Meeting on Agricultural Drought Indices, 2-4 June 2010, Murcia, Spain: Geneva, Switzerland: World Meteorological Organization. AGM-11, WMO/TD No. 1572; WAOB-2011. 219 pp.

Song, X., Huang, S., Qinhuo, L., & Xiaotao, L. (2007). Vegetation water inversion using MODIS satellite data. In 2007 IEEE International Geoscience and Remote Sensing Symposium (pp. 1865-1868). IEEE. https://doi.org/10.1109/IGARSS.2007.4423187.

Srivastava, A., Jain, S., Maity, R., Desai, V.R., 2022b. Demystifying artificial intelligence amidst sustainable agricultural water management. Current Directions in Water Scarcity Research 7, 17–35. https://doi.org/10.1016/B978-0-323-91910-4.00002-9.

Srivastava, A., Maity, R., Desai, V.R., 2022a. Assessing Global-Scale Synergy Between Adaptation, Mitigation, and Sustainable Development for Projected Climate Change. In: Chatterjee, U., Akanwa, A.O., Kumar, S., Singh, S.K., Dutta Roy, A. (Eds.), Ecological Footprints of Climate Change . Springer Climate. Springer, Cham. https://doi.org/10.1007/978-3-031-15501-7_2.

Suman, M., Maity, R., 2019. Assessment of streamflow variability with upgraded hydroclimatic conceptual streamflow model. Water Resour. Manag. 33 (4), 1367–1382. https://doi.org/10.1007/s11269-019-2185-8.

Swain, S.S., Mishra, A., Sahoo, B., Chatterjee, C., 2020. Water scarcity-risk assessment in data-scarce river basins under decadal climate change using a hydrological modelling approach. J. Hydrol. 590, 125260 https://doi.org/10.1016/j.jhydrol.2020.125260.

Swain, S.S., Mishra, A., Chatterjee, C., Sahoo, B., 2021. Climate-changed versus land-use altered streamflow: A relative contribution assessment using three complementary approaches at a decadal time-spell. J. Hydrol. 596, 126064 https://doi.org/10.1016/j.jhydrol.2021.126064.

Tennant, D.L., 1976. Instream flow regimens for fish, wildlife, recreation and related environmental resources. Fisheries 1 (4), 6–10. https://doi.org/10.1577/1548-8446(1976)001%3C0006:IFRFFW%3E2.0.CO;2.

Van Dijk, A.I., Beck, H.E., Crosbie, R.S., De Jeu, R.A., Liu, Y.Y., Podger, G.M., et al., 2013. The Millennium Drought in southeast Australia (2001–2009): Natural and human causes and implications for water resources, ecosystems, economy, and society. Water Resour. Res. 49 (2), 1040–1057. https://doi.org/10.1002/wrcr.20123.

Vandana, K., Islam, A., Sarthi, P.P., Sikka, A.K., Kapil, H., 2019. Assessment of potential impact of climate change on streamflow: a case study of the Brahmani River basin, India. J. Water Clim. Change 10 (3), 624–641. https://doi.org/10.2166/wcc.2018.129.

Vicente-Serrano, S.M., Beguería, S., López-Moreno, J.I., 2010. A multiscalar drought index sensitive to global warming: the standardized precipitation evapotranspiration index. J. Clim. 23 (7), 1696–1718. https://doi.org/10.1175/2009JCLI2909.1.

Vicente-Serrano, S.M., Quiring, S.M., Pena-Gallardo, M., Yuan, S., Dominguez-Castro, F., 2020. A review of environmental droughts: Increased risk under global warming? Earth Sci. Rev. 201, 102953 https://doi.org/10.1016/j.earscirev.2019.102953.

Wang, T., Tu, X., Singh, V.P., Chen, X., Lin, K., Lai, R., Zhou, Z., 2022. Socioeconomic drought analysis by standardized water supply and demand index under changing environment. J. Clean. Prod. 347, 131248 https://doi.org/10.1016/j.jclepro.2022.131248.

West, H., Quinn, N., Horswell, M., 2019. Remote sensing for drought monitoring & impact assessment: Progress, past challenges and future opportunities. Remote Sens. Environ. 232, 111291 https://doi.org/10.1016/j.rse.2019.111291.

Yang, X., Zhou, B., Xu, Y., Han, Z., 2021. CMIP6 evaluation and projection of temperature and precipitation over China. Adv. Atmos. Sci. 38, 817–830. https://doi.org/10.1007/s00376-021-0351-4.

Yin, J., Gentine, P., Slater, L., Gu, L., Pokhrel, Y., Hanasaki, N., et al., 2023. Future socio-ecosystem productivity threatened by compound drought–heatwave events. Nat. Sustainability 6 (3), 259–272. https://doi.org/10.1038/s41893-022-01024-1.

Zeydalinejad, N., Dehghani, R., 2023. Use of meta-heuristic approach in the estimation of aquifer's response to climate change under shared socioeconomic pathways. Groundw. Sustain. Dev. 20, 100882 https://doi.org/10.1016/j.gsd.2022.100882.